PAPER

Check for updates

Synthesis, thermophysical characterization and thermal performance analysis of novel Cu-MXene hybrid nanofluids for efficient coolant applications†

Kodi Rajesh Kumar and Aabid Hussain Shaik [ID] *

Hybrid nanofluids are considered as an alternative for conventional heat transfer fluids and mono nanofluids due to its remarkable enhancement in thermo-physical properties. However, there are some limitations in achieving the better thermo-physical properties due to the stability of nanoparticles in different base fluids at higher concentration. This work aims at synthesizing, thermo-physical characterization and thermal performance estimation of stable Cu-MXene based hybrid nanofluids using various base fluids at very low volume concentration of Cu and MXene nanostructures. Two step method is employed to prepare Cu-MXene hybrid nanofluids by dispersing the low volume concentration of as prepared Cu and MXene nanostructures (ranging from 0.01–0.05 vol%) containing SDS surfactant in various base fluids such as water, methanol, castor oil and silicon oil. Synthesized mono and hybrid nanofluids shows excellent stability against aggregation up to 7 days as evidenced from higher zeta potential values. Wettability studies conducted using contact angle measurement suggests that the castor oil, methanol and silicon oil based hybrid nanofluids exhibits hydrophilic behavior (showing contact angle less than 90°). Hybrid nanofluids display excellent enhancement in thermal conductivity at very low concentration of nanostructures (more than 70% for methanol based Cu-MXene hybrid nanofluid). Viscosity of the silicone oil based hybrid nanofluids show a remarkable enhancement followed by water, methanol and castor oil based hybrid nanofluids. Thermal conductivity and viscosity of hybrid nanofluids are effectively validated with existing theoretical models. Moreover, specific heat and pumping power of the hybrid nanofluids with respect to volume concentration of nanostructures are determined using the existing theoretical equations. Thermal performance of hybrid nanofluids was successfully estimated using Figure of Merit (FOM) analysis and suggested the better heat transfer fluid for improving the heat transfer performance under laminar and turbulent flow conditions for efficient cooling applications.

1 Introduction

Over the past few decades, the performance of heat exchangers has been steadily enhanced due to the advancement in the field of thermal engineering. Various conventional heat transfer fluids such as water, mineral oils, ethylene glycol *etc.* were used in several industrial operations such as power generation, chemical processes, heating and cooling processes, transportation, microelectronics to improve the performance of heat exchanging devices.[1,2] However, further enhancement in thermal performance was achieved by the dispersion of nano sized solid particles (<100 nm) in base fluids. These types of fluids are termed as "nanofluids".[3] Nanofluids provide excellent heat

transfer features such as high thermal conductivity and homogeneity due to small size and large specific surface areas of nanoparticles.[4] Due to this unique property, many researchers used nanofluids in a variety of technical applications.[5]

However, an outstanding enhancement in thermophysical and rheological properties was not achieved using mono nanofluids. Hence, more attention has been created in the research community to develop a new class of nanofluid such as "hybrid nanofluid" where two or more different types of nanoparticles dispersed in the base fluid to further enhance the base fluid thermo-physical and rheological properties.[6] Despite tremendous properties of hybrid nanofluids as compared to mono nanofluids, maintaining the stability of mono and hybrid nanofluids is a challenging task. The aggregation of nanoparticles in the suspended state causes the nanofluid to become unstable.[7] The thermo-physical and rheological characteristics of mono and hybrid nanofluids such as thermal conductivity, density, specific heat, viscosity *etc.* are greatly influenced by its

Colloids and Polymers Research Group, School of Chemical Engineering, Vellore Institute of Technology, Vellore, Tamilnadu, 632014, India. E-mail: aabidhussain.s@vit.ac.in

stability.[8] Poor stability of mono and hybrid nanofluids results in the drop of thermal and rheological properties.[9]

Despite stability, synthesis of stable hybrid nanofluids for remarkable enhancement of thermo-physical properties is another interesting aspect. Addition of hybrid nanoparticles to conventional base fluids exhibits enormous enhancement in thermal conductivity due to increased "Brownian motion".[10] The thermal conductivity of hybrid nanofluids depends on several factors including the concentration of nanoparticles, the type of nanoparticles, the base liquid or composition of the base liquid.[11] Suresh et al. formulated Al_2O_3–Cu hybrid nano-composite based hybrid nanofluid using water as a base fluid and sodium lauryl sulphate (SLS) as a surfactant by varying the volume concentration of nanoparticles ranging from 0.1 to 2 vlo.% and claimed 12.11% enhancement in thermal conductivity for maximum concentration of nanoparticles (i.e. 2 vol%).[12] Abbasi et al. prepared hybrid Υ-Al_2O_3-MWCNT nanocomposite based hybrid nanofluid by solvothermal process using de-ionized water as base fluid and reported 14.75% enhancement in the thermal conductivity for 0.01 volume fraction of nanoparticles.[13] Baby and Ramaprabhu synthesized Ag/HEG water and Ag/HEG ethylene glycol based hybrid nanofluids and noticed 25% increase in thermal conductivity at 0.05% volume concentration of nanoparticles at 25 °C.[14] Nine et al. synthesized hybrid nanofluids using water as base fluid by ball milling technique with 95% Al_2O_3, 5% MWCNT and 90% Al_2O_3, 10% MWCNT and estimated the thermal conductivity at various particle concentrations.[15] Other properties such as density and specific heat also plays a major role in improving the heat transfer performance of various thermal systems as reported by other researchers.[16]

Moreover, viscosity of hybrid nanofluids also plays a vital role in evaluating pumping power requirements due to frictional effects. The "Newtonian or non-Newtonian" behavior of a fluid is characterized by measuring the viscosity of hybrid nanofluids.[17,18] Esfe et al. studied the rheological behavior of SAE 50 based MWCNT-Al_2O_3 hybrid nanofluid using the Brookfield viscometer at various volume concentrations and claim the non-Newtonian behavior.[19] Wanatasanappan et al. synthesized the water-EG based Al_2O_3–Fe_2O_3 hybrid nanofluids at different weight ratios of Al_2O_3 and Fe_2O_3 and shows the Newtonian fluid behavior by measuring viscosity using Brookfield viscometer.[20] Huminic et al. examined the viscosity of water-based Fe–Si hybrid nanofluids with respect to nanoparticle mass concentration and concluded that the viscosity elevates with increasing nanoparticle concentration.[21] Ilyas et al. identified the non-Newtonian i.e. shear thinning fluid behavior of graphene-based nanofluids in thermal oil.[22] Mostafizur et al. determined dynamic viscosity using viscometer for Al_2O_3-MWCNT/radiator coolant hybrid nanofluid for different volume fractions (0.1 to 0.5 vol%), temperature (20 to 60 °C) and revealed that viscosity increases with increase in volume fraction of nanoparticles and decreases with increase in temperature.[23]

In addition to thermal and rheological properties of hybrid nanofluids, it is important to recommend suitable hybrid nanofluids for different flow regimes (laminar and turbulent flow) in industrial cooling applications. This can be achieved using Figure of Merit (FOM) analysis. Figure of merit (FOM)

facilitates the characterization of the nanofluid performance in laminar and turbulent flows.[24] A very few works have been reported in the literature with respect to Figure of Merit analysis. Chakraborty et al. measured the overall thermal performance of TiO_2 nanofluid using FOM analysis and reported that the TiO_2 nanofluid shows better heat transfer capability in internal laminar flow and failed to show the improved performance in internal laminar flow conditions as per FOM data.[25] Elcioglu et al. 2020 claim that the FOM depend on a dimensionless number such as Mouromtseff number (Mo) and mentioned that thermal performance of hybrid nanofluid is better than base fluid for Mo number higher than unity.[26]

Wettability of nanofluid is an important characterization for better boiling heat transfer and is greatly affected by various surface properties, base fluid, particle concentration, and the type of surfactant. A limited work has been conducted on measuring wettability of nanofluids using contact angle measurements.[27–29] From the overview of the literature, most of the work has been conducted on synthesis of oxide based mono and hybrid nanofluids using water as base fluid by dispersing high concentration of particles in base fluid for enhancing the thermophysical properties. This oxide based materials shows better performance in other fields such as supercapacitor and LED applications other than cooling applications.[30–32] However, the enhancement in thermal conductivity is also not up to the mark (able to achieve less than 25%). Hence a development of cost effective novel and stable hybrid nanofluid with low concentration of nanoparticles in different base fluids for better enhancement of thermophysical properties is very much essential. This paper focuses on the synthesis of novel and stable MXene and Cu-MXene based mono and hybrid nanofluids using different base fluids such as water, methanol, castor oil and silicone using low concentration of nanoparticles for remarkable enhancement in thermophysical properties. Moreover, this work also emphases on measuring the thermal performance of hybrid nanofluid by exploring the suitability of hybrid nanofluids in different flow regimes using FOM analysis which is very sparse in the literature. The main reason for using Cu and MXene in this work, is, former is a noble cost effective metal and has high thermal conductivity which can be utilized by replacing expensive noble metals like silver and gold in several applications like optical, electrical etc.[33] On the other hand, MXenes are a rapidly expanding class of 2D layered like materials with exceptional thermal properties.[34]

2 Experiments

2.1. Materials required

Copper(II) chloride dihydrate ($CuCl_2 \cdot 2H_2O$) and hydrazine hydrate (N_2H_4) were purchased from Sigma-Aldrich, India. Ammonia solution (25%) was received from SD Fine Chemicals, India. Polyvinylpyrrolidone (PVP K-30) was obtained from SRL, India. Max phase Titanium aluminum carbide (TAC) was procured from Nanoshel, India. Absolute ethanol was supplied by Changshu Hongsheng fine chemicals, China. Base fluids such as methanol, silicone oil, and castor oil were brought from Loba chemie, India. Chemicals purchased were used in the synthesis process directly without performing any purification.

2.2. Deoxygenation of base fluid

Since copper is an easily oxidizing material, it is crucial to lower the amount of dissolved oxygen in the base fluid. All the base fluids used in the synthesis process were purged with nitrogen (N_2) gas for 30 minutes. After purging, the concentration of dissolved oxygen in the base fluids were reduced from 0.9 ppm to 0.3 ppm as measured by the dissolved oxygen (DO) meter.

2.3. Synthesis of Cu nanoparticles powder

Cu nanoparticles in aqueous phase were prepared by modifying the protocol published by Chowdhury et al.[35] Briefly, 5 g of PVP solution was prepared by adding 5 g PVP in 80 mL of deoxygenated distilled water under vigorous stirring. Later, the above solution was mixed with 0.272 g of copper chloride dihydrate and stirred continuously until the solution color changes to light blue. Then, the pH of the solution was adjusted to 10 to 11 by gradual addition of ammonia solution under vigorous stirring. The color of the solution immediately turns inkish blue and the above solution was stirred constantly at a temperature of 50 °C in a water bath for an hour. After 1 hour, 20 mL of 0.6 M hydrazine hydrate solution was prepared separately and added to the above solution. Subsequently, the color of the solution changes to transparent white, and nucleation begins slowly. Thereafter, the color of the solution changes from white to light brown followed by reddish brown, indicating the formation of copper nanoparticles in aqueous phase. Next, Cu nanopowder was prepared from the as synthesized aqueous Cu sol by centrifuging the sol at 10 000 rpm for 30 minutes. After 30 min, Cu nanoparticles accumulated at the bottom of the centrifuge tubes by leaving a clear supernatant. The accumulated Cu nanoparticle powder in the centrifuge tube is separated from the supernatant and dried using vacuum oven overnight at 60 °C. After drying, Cu nanoparticle powder was recovered from the centrifuge tubes.

2.4. Synthesis of Mxene Titanium carbide (TiC) layered nanosheets

Mxene titanium carbide (TiC) layered nanosheets were synthesized by following the procedure developed by Kumar et al.[34] In this method, initially, 2 g titanium aluminum carbide (TAC) was added to 50 mL of hydrofluoric acid (HF) followed by continuous agitation for 24 hours at 50 °C. Later, the product was recovered by ethanol and DI water washing for multiple times. Then, it is subjected to 24 h freeze drying process to obtain black powder. Thereafter, 1 g of as synthesized TiC powder was dissolved in 20 mL of dimethyl sulfoxide (DMSO) and stirred at ambient temperature for 18 h under inert environment. Finally, the black product was then dried overnight at 80 °C in a vacuum oven after being rinsed with DI water/ethanol.

2.5. Synthesis of MXene and Cu-Mxene based mono and hybrid nanofluids

MXene and Cu-MXene mono and hybrid nanofluids were prepared by dispersing the already synthesized Cu and MXene nanopowders in base fluid using ultra-sonication technique. For preparing MXene mono nanofluid, the weights of different volume concentrations of MXene (0.01, 0.015, 0.02, 0.04 and 0.05%) powder were weighed separately and mixed with various base fluids such as water, methanol, castor oil and silicone oil containing SDS surfactant using magnetic stirrer for 20 min followed by probe type ultra-sonication for 1 hour. The same procedure is followed for synthesizing Cu-MXene hybrid nanofluid by adding 0.01 vol% of Cu nanoparticle powder along with MXene powder in various base fluids. Cu nanoparticle powder concentration was kept constant at 0.01 vol% in all the samples of hybrid nanofluids by varying MXene concentration (0.01, 0.015, 0.02, 0.04 and 0.05%).

2.6. Thermal conductivity measurement of hybrid nanofluid

Thermal conductivity of mono and hybrid nanofluids was measured using KD2 Pro thermal conductivity meter (Decagon Devices Inc). It consists of a small single needle (KS-1) sensor with a length of 6 cm and will be used to measure thermal conductivity from 0.02 to 2 W m^{-1} K^{-1} range. The probe was placed in the fluid for 20 minutes without disturbing to reach the steady state. The fluid is remained stable and immobile by placing the sample in a jacketed oil bath in order to reduce thermal convection of mono and hybrid nanofluids during thermal conductivity measurement. Finally, the thermal conductivity readings were repeated thrice, and the average values were reported.

2.7. Density measurement of mono and hybrid nanofluids

Specific gravity bottle (or) density bottle is used to measure the densities of mono and hybrid nanofluids. This method is simple and measured by estimating the ratio of the difference between empty bottle and fluid filled bottle with equal volume of base fluid. This gives the specific gravity of liquid which can be used to calculate the density by multiplying with density of base fluid at standard conditions.

2.8. Viscosity measurement of hybrid nanofluids

The viscosity of hybrid nanofluids was measured using the DV2TLV AMETEK Brookfield viscometer (USA), which consists of a small chamber with 0.750 inch diameter and 2.55 inch depth. The fluid viscosity was evaluated using several spindles by varying the RPM of the spindle. The viscosity of the synthesized hybrid nanofluids was investigated using a cylindrical spindle with variable RPM. A jacketed oil bath (Brookfield, TC 550) is employed to maintain a temperature consistent during the measurement of the sample.

2.9. Wettability of hybrid nanofluids

Contact angle measurements were performed to observe the wettability behavior of different fluids on plain surfaces. In this work, a cast iron plate has been considered as a plain surface over which drop of the hybrid nanofluid was placed to measure the contact angle using drop shape analysis method (DSA25B model, Germany). After the drop casting of hybrid nanofluid on the surface of a cast iron plate, a photo of the droplet and the angle created by the liquid–surface interface to the liquid–air

interface was measured using a high-speed camera (CF06), with a frame rate of 3400 fps.

2.10. Characterization

The characterization of the mono and hybrid nanofluids was performed using a variety of techniques. The optical properties of mono and hybrid nanoparticles were measured using UV-vis spectrophotometer (SHIMADZU 1800). The morphology of Cu and MXene nanostructures were characterized using Transmission Electron Microscope (Technai G2 20S Twin) and Field Emission Scanning Electron Microscope (FESEM, ZEISS). Energy dispersive X-ray (EDX) spectroscopy is used to analyze the elemental composition Cu and MXene nanostructures. The stability of mono and hybrid nanofluids was examined using dynamic light scattering equipment (HORIBA SZ-100, version 2.00) by measuring the zeta potential with respect to time. The phase purity of Cu and MXene nanostructures was characterized using X-ray diffraction (XRD) with Cu-Kα radiation (Bruker D8 Advance, Germany). Atomic force microscopy (Nanosurf AG Switzerland, model no: 23-06-154) is used to measure the thickness of MXene layered sheets. The functional groups of MXene and Cu nanostructures are characterized using Fourier Transform Infrared spectroscopy (Thermo Nicolet iS50 with inbuilt ATR, Thermo Fisher Scientific, USA). Surface chemical composition of the nanostructures are analyzed using Raman spectroscopy (Anton Paar GmbH, model Cora 5001). The contact angle of mono and hybrid nanofluids in different base fluids was obtained using Goniometer.

3 Results and discussion

3.1. Synthesis of mono and hybrid nanofluids

Hybrid nanofluids displays remarkable enhancement in thermal and rheological properties of the based fluids as compared to mono nanofluids. However, there are some challenges which need to overcome before using these hybrid
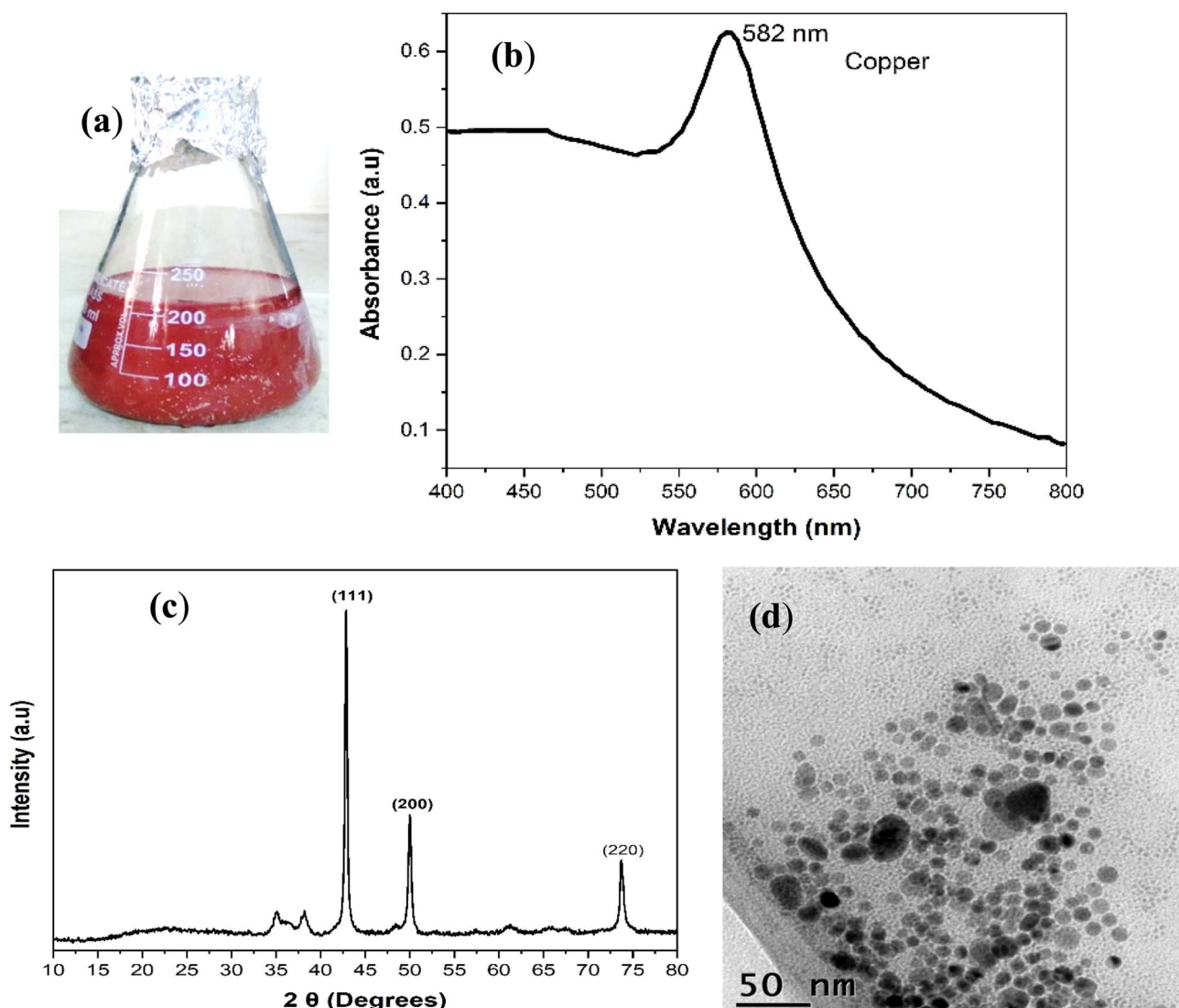

Fig. 1 (a) Digital photo image (b) UV-vis (c) XRD and (d) TEM image of Cu nanoparticles.
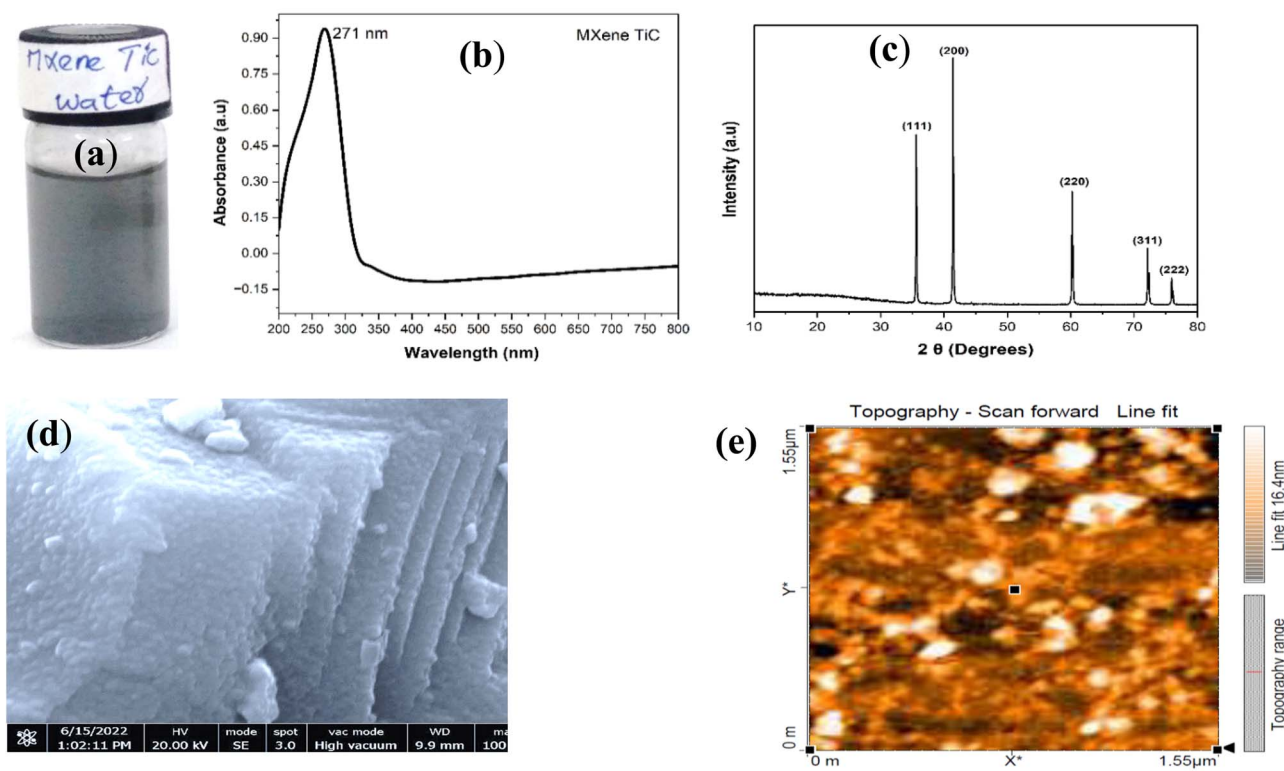
Fig. 2   (a) Digital photo image (b) UV-vis (c) XRD (d) FESEM and (e) AFM surface image of MXene nanosheets.
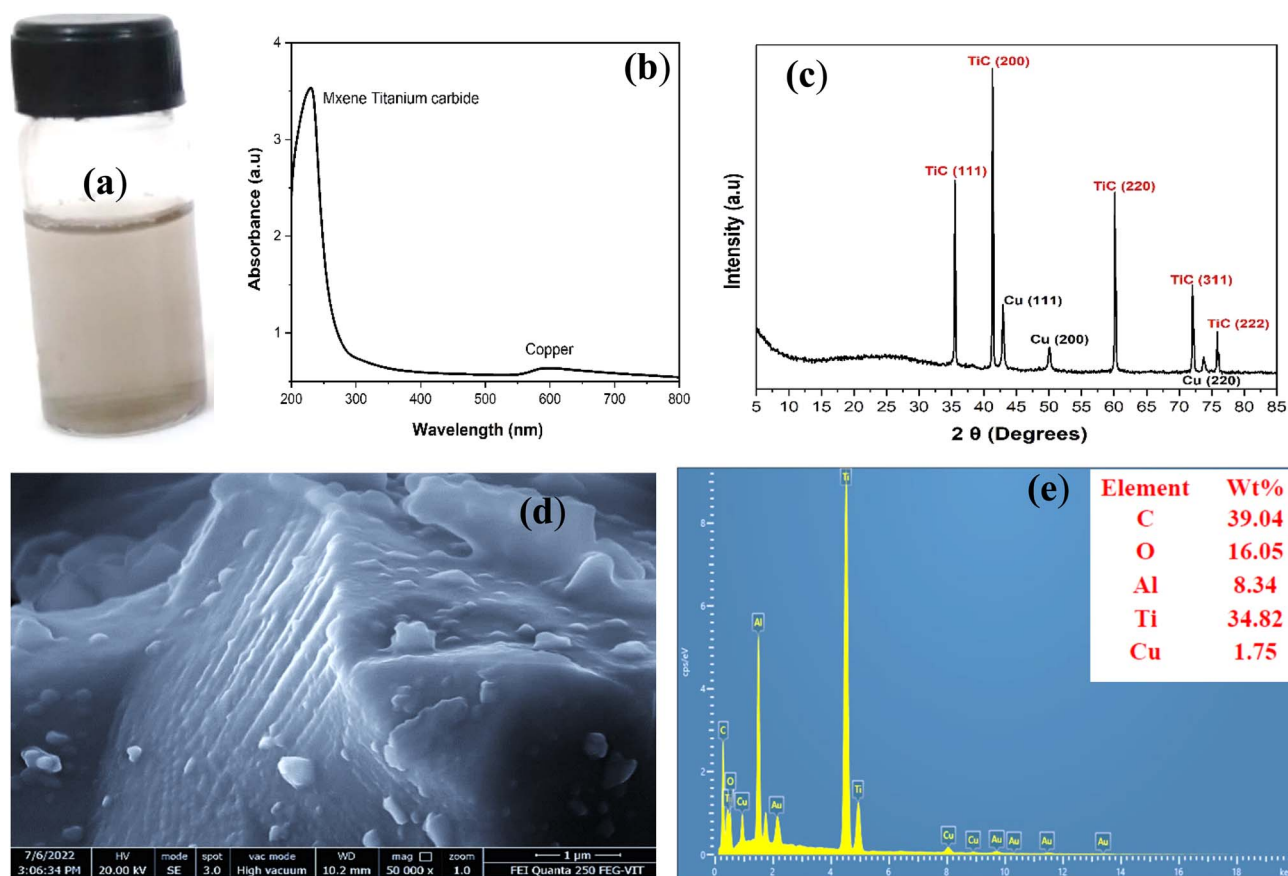

Fig. 3   (a) Digital photo image (b) UV-vis (c) XRD (d) FESEM and (e) EDX of Cu-MXene water based hybrid nanofluid.
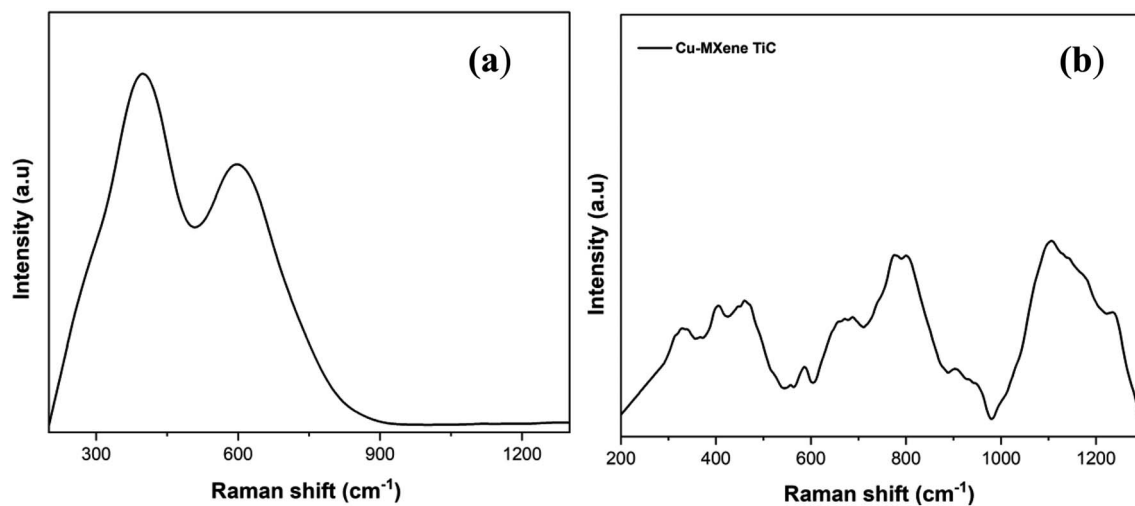
Fig. 4   Raman spectra of (a) MXene and (b) Cu-MXene nanostructures.

nanofluids for cooling applications. One of the major challenges is the stability of hybrid nanofluids due to the suspension of two different types of nanoparticles in the base fluid. In

this work, Cu-MXene based hybrid nanofluids were prepared by suspending the as prepared Cu nanoparticles and layered MXene nanosheets in different base fluids such as water,
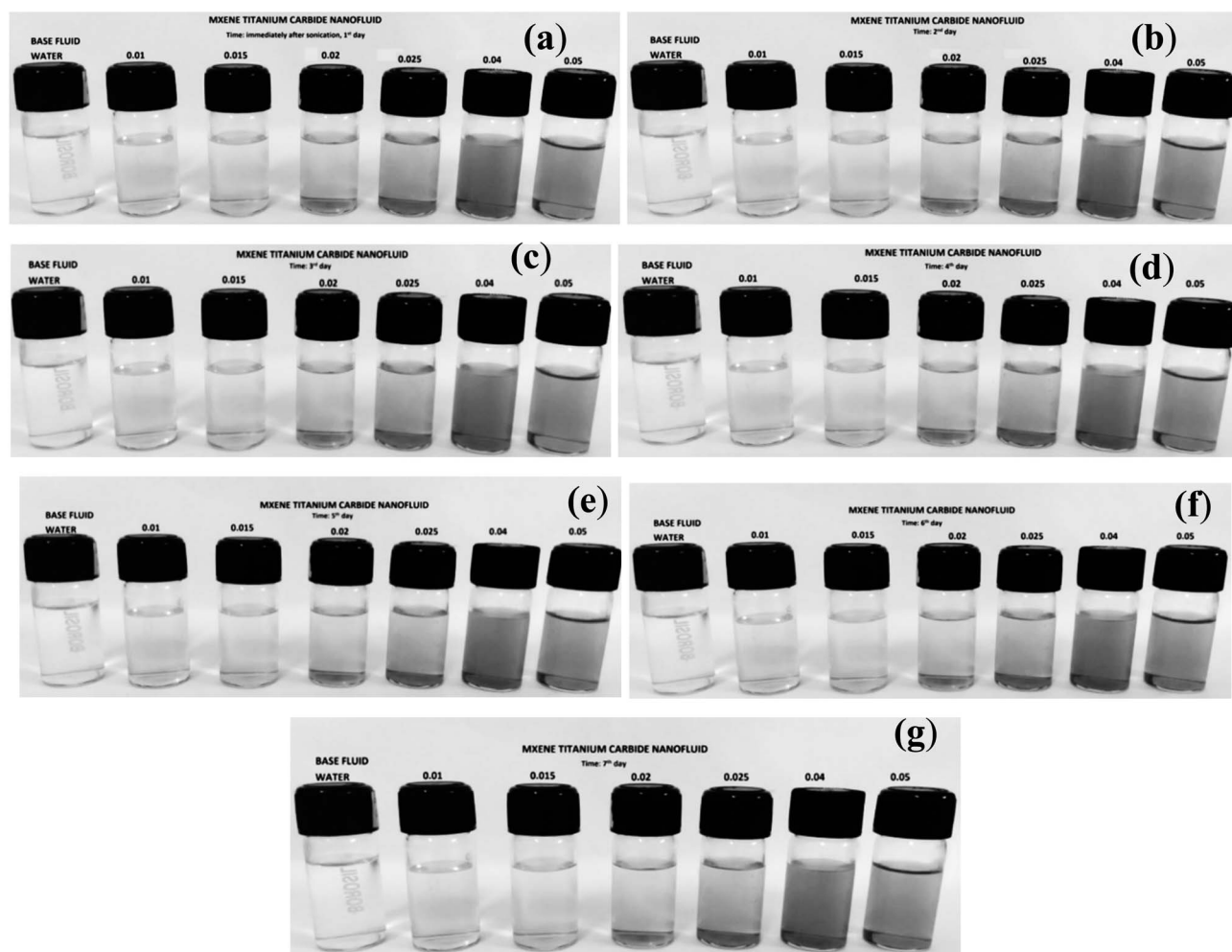

Fig. 5   Stability analysis of water based MXene nanofluids through visual inspection: (a) after preparation (b) after 2 days (c) after 3 days (d) after 4 days (e) after 5 days (f) after 6 days (g) after 7 days.

methanol, castor oil and silicone oil. Since, the Cu is an easily oxidizable material; there is a substantial chance of oxidation of nanoparticles in the hybrid nanofluid in addition to stability associated due to aggregation. Moreover, MXene also pose a major threat in terms of oxidation stability even though it shows better hydrophilic properties and thereby results in the forfeiture of thermal properties of MXene. Hence, a confined oxygen free environment has been created in the current work in order to make the Cu-MXene hybrid nanofluids stable against oxidation and aggregation so that it can be used in various industrial cooling applications as a coolant.

First, Cu nanoparticles and MXene layered nanosheets were synthesized separately and used for preparing Cu-MXene based hybrid nanofluids using different base fluids. Fig. 1 represents the optical, morphological and phase behavior of the Cu nanoparticles. The digital image showed in Fig. 1(a) represents the suspension of Cu nanoparticles in water. From the image, it can be seen that the suspension shows reddish brown color without any sign of oxidation indicating the Cu particles highly stable against oxidation and aggregation. This was further

confirmed by the UV-vis and XRD analysis as shown in Fig. 1(b) and (c). UV-vis analysis from Fig. 1(b) shows a characteristic surface plasmon resonance peak at 582 nm signifying the formation of strong oxidation and aggregation resistant Cu nanoparticles. After the preparation of Cu nanoparticle suspension, Cu nanoparticle powder was produced by centrifuging and drying the paste obtained after centrifugation. The phase purity of cu nanoparticles obtained from the XRD analysis shown in Fig. 1(c) also reveals that the particles are stable against oxidation as observed from the diffraction peaks at 42.8, 49.9, and 73.6 which corresponds to the 111, 200 and 220 planes of face-centered-cubic (fcc) crystal structure of Cu as confirmed by Chowdhury *et al.*[35] and JCPDS: 00-004-0836. Moreover, the particles are well separated and spherical in nature with a size of ∼20 nm as noticed from TEM image shown in Fig. 1(d). SEM analysis is also conducted to observe the morphology of Cu nanoparticles and shown in the ESI as Fig. S1.† From the SEM image, it has been observed that the Cu nanoparticles are polydisperse in nature and raging the size from 10–40 nm and display a mean size of ∼30 nm. In addition EDX analysis is also
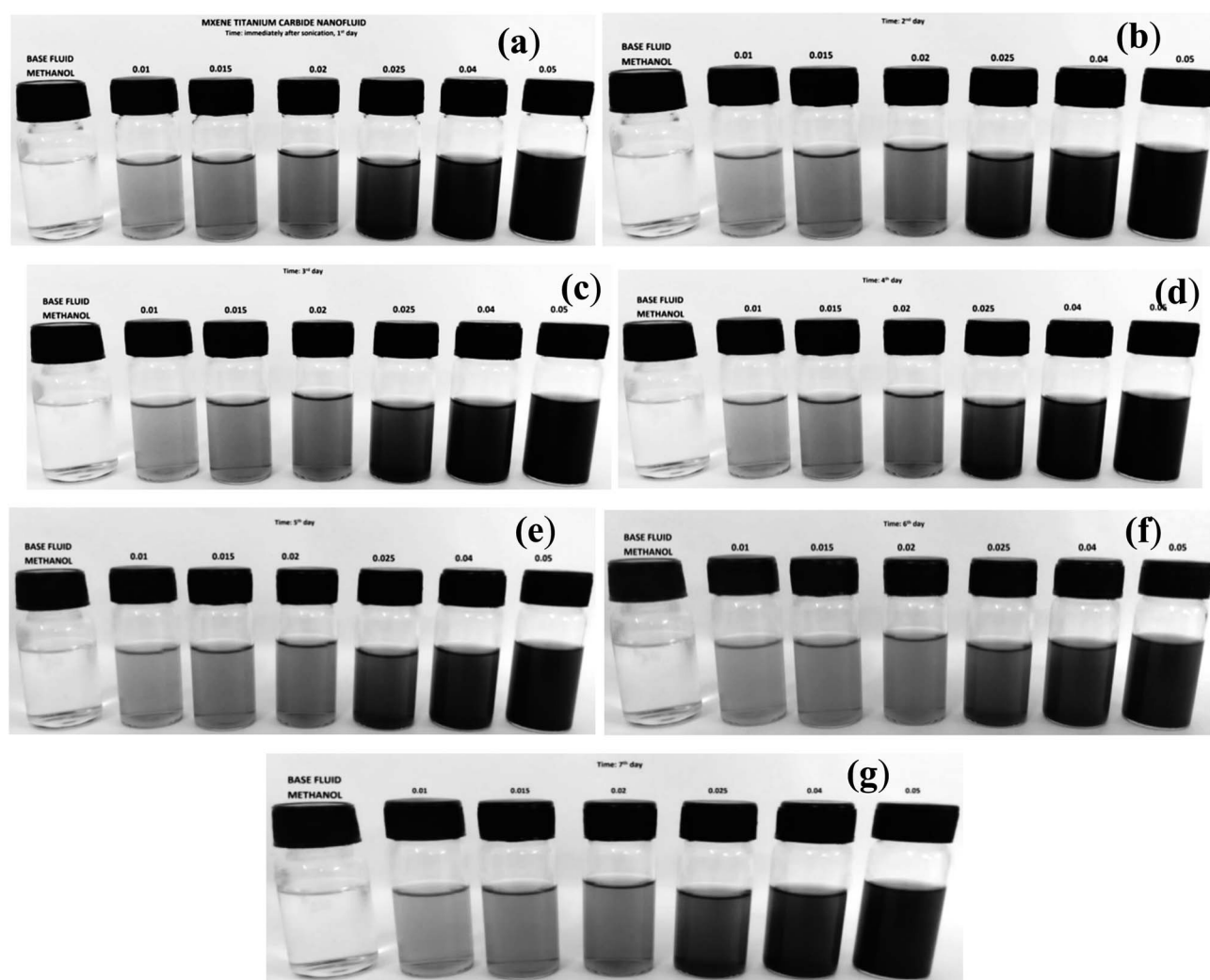

Fig. 6 Stability analysis of methanol based MXene nanofluids through visual inspection: (a) after preparation (b) after 2 days (c) after 3 days (d) after 4 days (e) after 5 days (f) after 6 days (g) after 7 days.

conducted to detect the chemical composition of Cu nano-particles and shown in Fig. S2.† EDX shows the peaks of Cu along with a slight oxide peak which may be due to surface oxidation of Cu nanoparticles.

Next, MXene nanosheets were synthesized successfully by modifying the already reported hydrofluoric acid (HF) etching method. Fig. 2(a) represents the suspension of MXene nano-sheets in water indicating the characteristic black color of MXene in the suspension. UV-vis analysis of MXene nanosheets suspension shown in Fig. 2(b) shows a surface plasmon reso-nance peak at ∼271 nm which corresponds to the characteristic peak of MXene nanosheets. The presence of the peak at 271 nm designate that the MXene nanosheets are successfully prepared in water and maintained in well stable nature against aggrega-tion. Further confirming the presence of MXene nanosheets in suspension, XRD analysis of the MXene layered nanosheets powder obtained after the centrifugation and drying of the suspension was performed and shown in Fig. 2(c). From the XRD data, several diffraction peaks were observed at different diffraction angles 35.6, 41.4, 60.2, 72.1, and 75.9 which

corresponds to the 111, 200, 220, 311, and 222 planes of face-centered-cubic (fcc) crystal structure of MXene as confirmed by Kumar *et al.* (2020)[34] and JCPDS No: 00-031-1400. This confirms that the synthesized material is a MXene nanosheet without any presence of other material. The morphology of MXene nanosheets was further examined using the FESEM characterization as shown in Fig. 2(d). FESEM image shows that the MXene nanosheets are representing the 2D multilayered sheet-like structure. AFM image shown in Fig. 2(e) exhibits a thickness of ∼20 nm.

After successful preparation of individual Cu and MXene nanostructures, Cu-MXene based hybrid nanofluid was prepared by dispersing the required volume concentrations of Cu and MXene nanostructure powders in different base fluids containing the surfactant using ultra sonication. Fig. 3(a) signifies the digital photo image of Cu-MXene based hybrid nanofluid synthesized using water as base fluid. From the digital image, it has been observed that he hybrid nanofluid is stable against aggregation as confirmed from the non-settling of particles at the bottom of the vial. The presence of stable
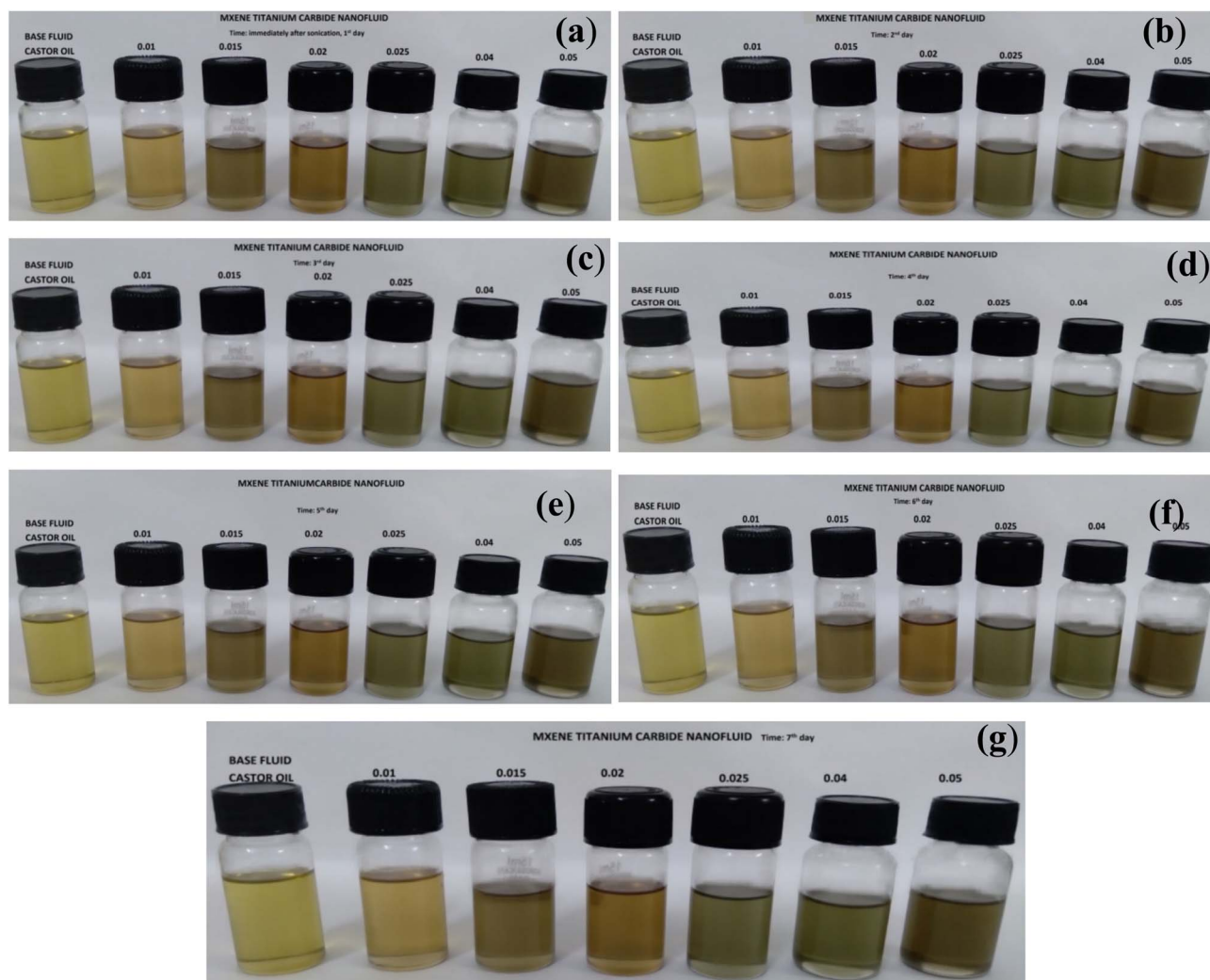

Fig. 7 Stability analysis of castor oil based MXene nanofluids through visual inspection: (a) after preparation (b) after 2 days (c) after 3 days (d) after 4 days (e) after 5 days (f) after 6 days (g) after 7 days.
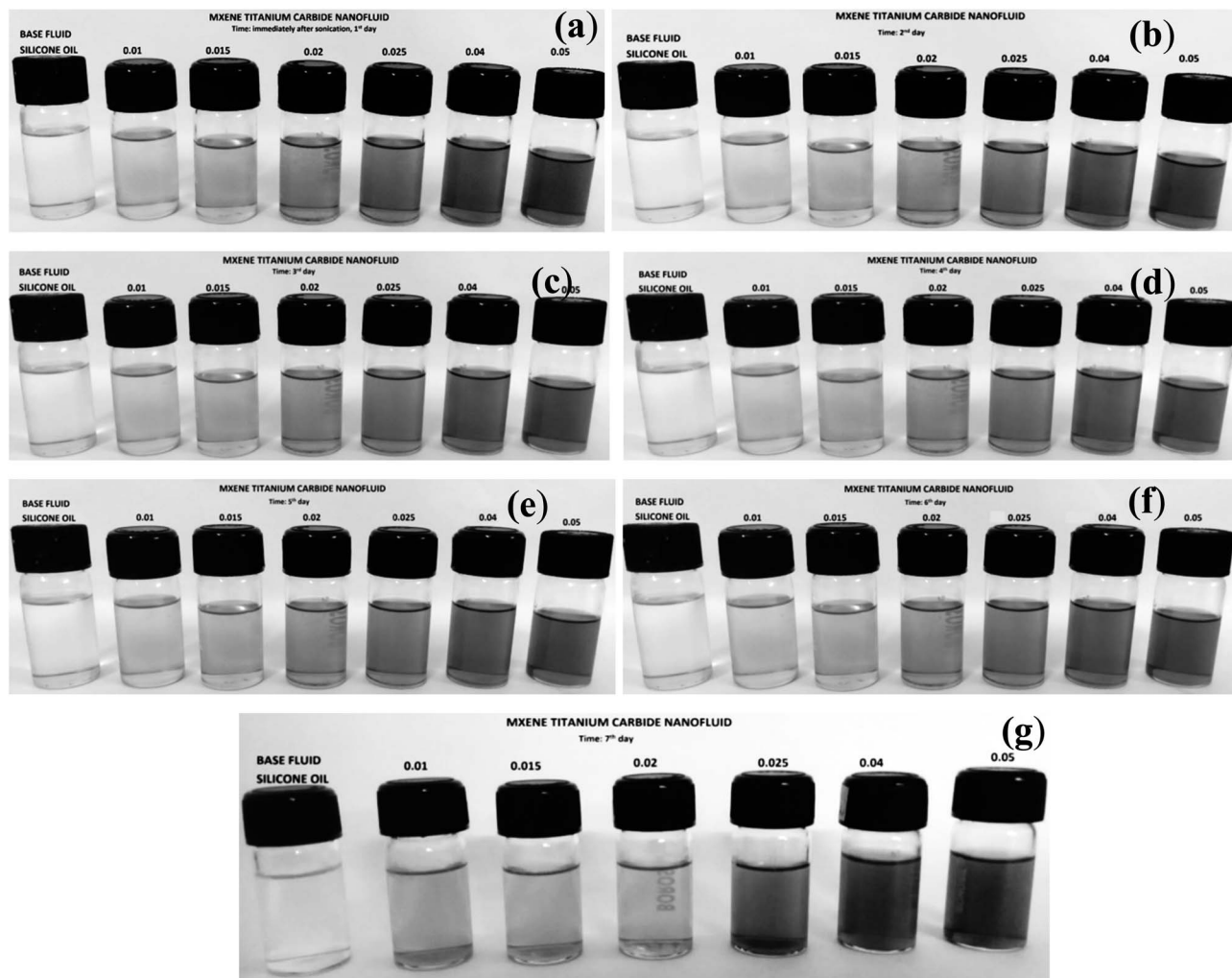
Fig. 8 Stability analysis of silicon oil based MXene nanofluids through visual inspection: (a) after preparation (b) after 2 days (c) after 3 days (d) after 4 days (e) after 5 days (f) after 6 days (g) after 7 days.

suspension of hybrid nanofluid was further confirmed by the UV-vis analysis as shown in Fig. 3(b). UV-vis of Cu-MXene hybrid nanofluid shows the characteristic surface plasmon resonance peaks of both Cu and MXene confirming the stability of hybrid nanofluid in water. The phase purity of hybrid nanostructures was also characterized by conducting the XRD analysis of the hybrid nanopowder as shown in Fig. 3(c). From the XRD data, it has been observed that the hybrid nanopowder contains the traces of both Cu and MXene diffractions peaks at different diffraction angles corresponding to fcc planes of Cu and MXene (JCPDS: 00-004-0836 and JCPDS No: 00-031-1400) suggesting the formation of hybrid structure in the sample. The morphology of hybrid nanostructures present in the hybrid nanofluid was observed using the FESEM analysis shown in Fig. 3(d). Two dimensional layered MXene nanosheet structure along with spherical Cu nanoparticles deposited on the layered MXene were observed in the sample indicating the successful formation of hybrid Cu-MXene nanostructure. The presence of Cu traces along with Ti and C traces are also confirmed by the EDAX conducted on the sample as shown in Fig. 3(e).

Moreover, the functional groups present in synthesized MXene and Cu-MXene nanostructures are identified using FTIR analysis and shown in Fig. S3 of ESI.† From the Fig. S3(a),† broad peaks detected at 2565 cm^{-1} and 1492 cm^{-1} suggest the stretching vibrations of C–F bond that emerge due to the usage of HF during etching process of MXene preparation. Moreover, N–H stretching, hydroxyl groups (O–H) and carboxyl C=O stretching are identified at 3628 cm^{-1} 2930 cm^{-1} and 1768 cm^{-1} bands respectively. C–H groups are also detected at 1492 cm^{-1} and 1058 cm^{-1} along with NH$_2$ bond spotted at 2160 cm^{-1} and 2022 cm^{-1}. FTIR spectra of hybrid Cu-MXene nanostructure shown in Fig. S3(b)† exhibit O–H bond at 3750 cm^{-1} along with other groups such as Cu–OH and Ti–OH at 957 cm^{-1} and 490 cm^{-1}. The functional groups present in MXene and Cu-MXene are in consistent with the literature.[36–39]

3.1.1 Surface characterization of MXene and Cu-MXene nanostructures using Raman spectroscopy. Raman spectroscopy is used to identify the surface composition of materials. In this work, Raman spectroscopy is used to observe the surface chemical composition of MXene and Cu-MXene nanostructures
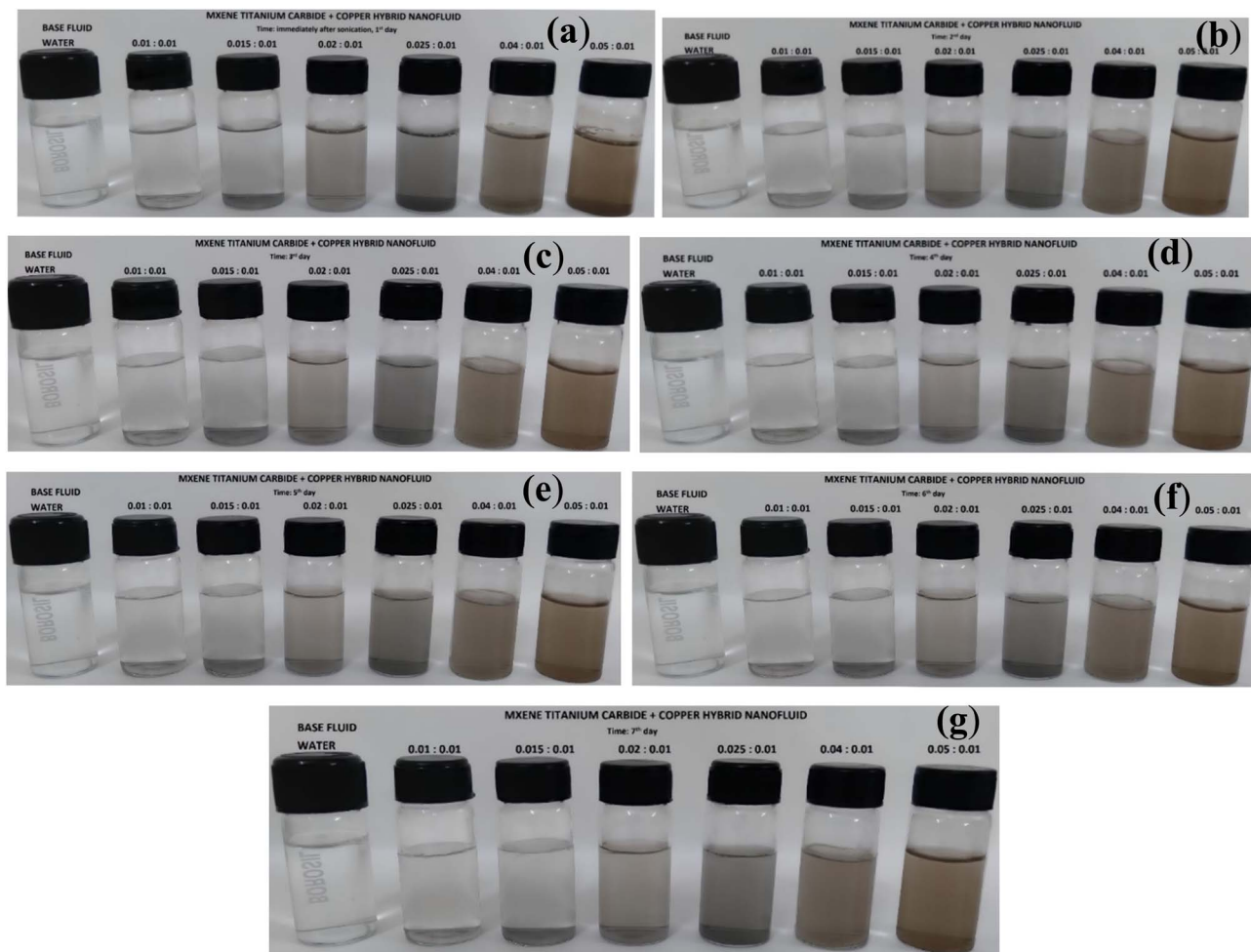
Fig. 9 Stability analysis of water based Cu–MXene hybrid nanofluids through visual inspection: (a) after preparation (b) after 2 days (c) after 3 days (d) after 4 days (e) after 5 days (f) after 6 days (g) after 7 days.

through molecular vibrations and shown in Fig. 4. Raman spectra of MXene shown in Fig. 4(a) represents a peak at 720 cm^{-1} correspond to A_{1g} (Ti, C) vibrational mode of MXene. Another peak observed at 375 cm^{-1} resembles the typical E_{1g} vibrational mode accompanying with the functional surface oxide form of TiC due to the possible surface oxidation of MXene upon exposure to air. Moreover, Raman spectra of Cu-MXene shown in Fig. 4(b) exhibit both peaks of MXene (720 cm^{-1}) and Cu (300 cm^{-1}, 640 cm^{-1} and 800 cm^{-1}) in oxide form due to surface oxidation of Cu indicating the formation of Cu-MXene hybrid composite. These results are in consistent with the other works reported in literature.[40,41]

3.2. Stability of mono and hybrid nanofluids

MXene nanofluids and Cu-MXene hybrid based nanofluids are successfully synthesized in various base fluids such as methanol, silicone oil and castor oil by following the same procedure as adopted for water base fluid. Even though, the mono and hybrid nanofluids are successfully synthesized, maintaining the stability of mono and hybrid nanofluids becomes a challenging task. In the current work, mono and hybrid nanofluids were protected against aggregation by dispersing the surfactant such as SDS in the mono and hybrid nanofluid. After successful incorporation of surfactant, stability analysis was effectively conducted by visual observation and measuring zeta potential with respect to time. Fig. 5 represents the digital photo images of water based MXene mono nanofluids synthesized by varying MXene concentrations (0.01, 0.015, 0.02, 0.025, 0.04 and 0.05 vol%) with respect to time ranging from 1 to 7 days showing the excellent stability of nanofluids against aggregation. These nanofluids do not show any sign of sedimentation of MXene particles in all the concentrations even though the nanofluid is stored in a vial for one week.

Stability of methanol based MXene nanofluids with various MXene concentrations (0.01, 0.015, 0.02, 0.025, 0.04 and 0.05 vol%) were also examined with respect to time by keeping the nanofluid in the vial without disturbing and digital photo images are captured with respect to time for possible notice of the sedimentation of particles as shown in Fig. 6. From the figure, it has been observed that the methanol based nanofluids are highly stable for at least one week as confirmed from the digital photo images showing no traces of sedimented particles in the vial.

Visual inspection of castor oil based nanofluids prepared with different MXene concentrations (0.01, 0.015, 0.02, 0.025, 0.04 and 0.05 vol%) with respect to time is shown in Fig. 7. In this nanofluid, surfactant such as SDS was not added to make the nanofluid stable as it was added in water and methanol based nanofluids. Even though there is no surfactant, particles are highly stable in castor oil due to the presence of triglyceride (which contains 18 carbon chains) in its structure. Nanofluid is stable even after one week without any traces of settled MXene particles in the vial.

Suspension of MXene particles in silicone oil also shows the same remarkable stability as it was observed in castor oil as shown in Fig. 8. MXene is also highly stable in silicone oil even without the presence of surfactant due to siloxane group present in the structure as observed from the digital images shown in Fig. 8. The siloxane in its structure creates a steric hindrance in holding the particles and thereby allowing the particles to stay away from each other. Nanofluid do not show any traces of settling of particles even after 7 days. This confirms that the MXene nanoparticles are highly stable in silicone oil.

Next, Cu-MXene based hybrid nanofluids stability was also observed visually for possible sedimentation of nanoparticles in the vial with respect to time. Water based Cu-MXene hybrid nanofluid suspension (prepared by varying MXene concentration and keeping Cu concentration constant) was sonicated rigorously for about 45 min in the presence of SDS surfactant to improve the stability. After 45 min, all six samples of water based Cu-MXene hybrid nanofluid stability was monitored visually for possible settling of particles with respect to time for 7 days as shown in Fig. 9. From the figure, it can be seen that the hybrid nanofluid suspension is highly stable even after 7 days without aggregation of particles in the vial.

Cu-MXene hybrid nanofluids also show outstanding stability against aggregation in methanol base fluid as shown in Fig. 10. The visual observation of six different samples of hybrid nanofluids containing MXene and Cu nanoparticle concentrations (vol%) ratio (0.01 : 0.01, 0.015 : 0.01, 0.02 : 0.01, 0.025 : 0.01, 0.04 : 0.01 and 0.05 : 0.01) confirms that the hybrid nanofluid suspension is highly stable for at least 7 days
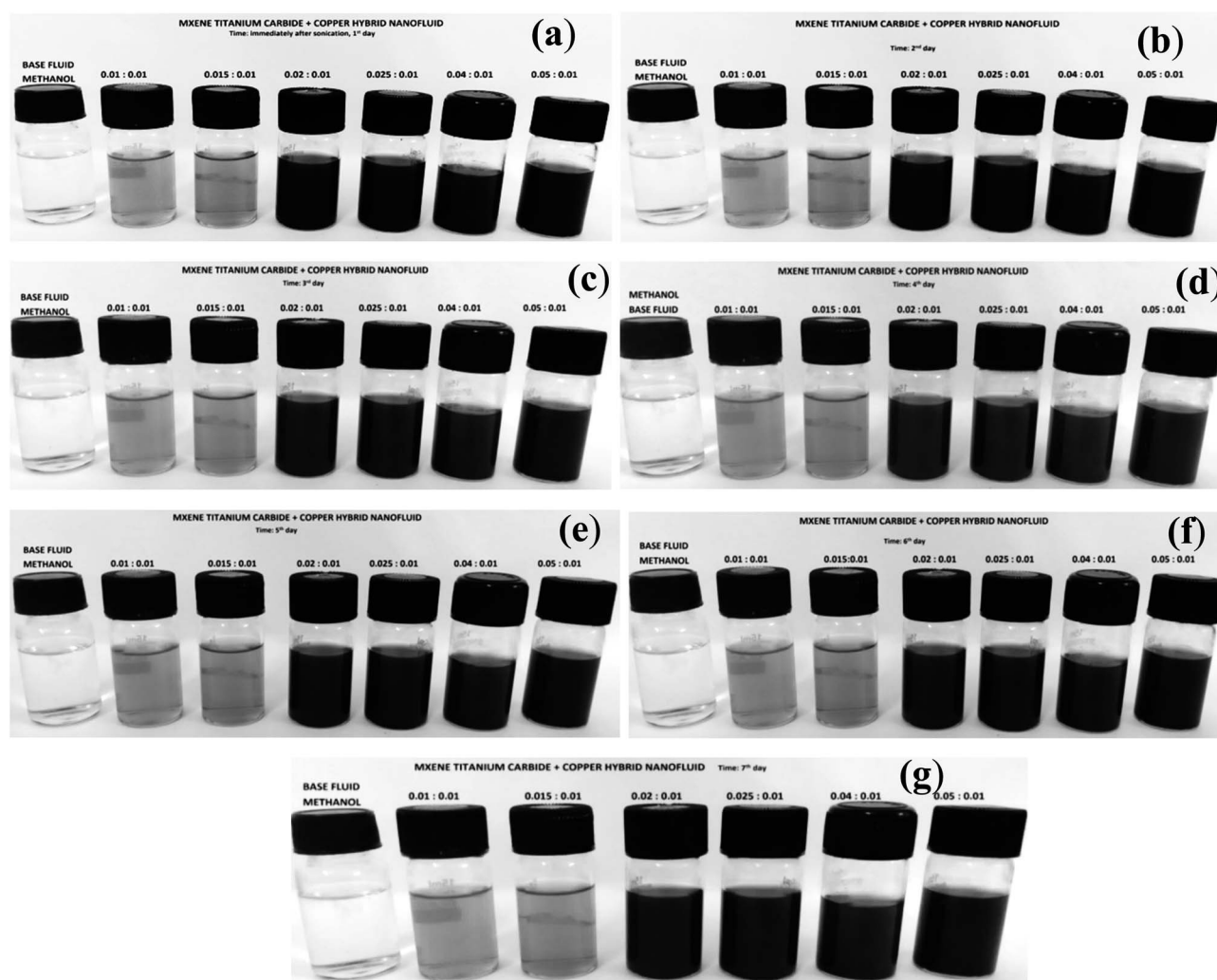

Fig. 10 Stability analysis of methanol based Cu- MXene hybrid nanofluids through visual inspection: (a) after preparation (b) after 2 days (c) after 3 days (d) after 4 days (e) after 5 days (f) after 6 days (g) after 7 days.
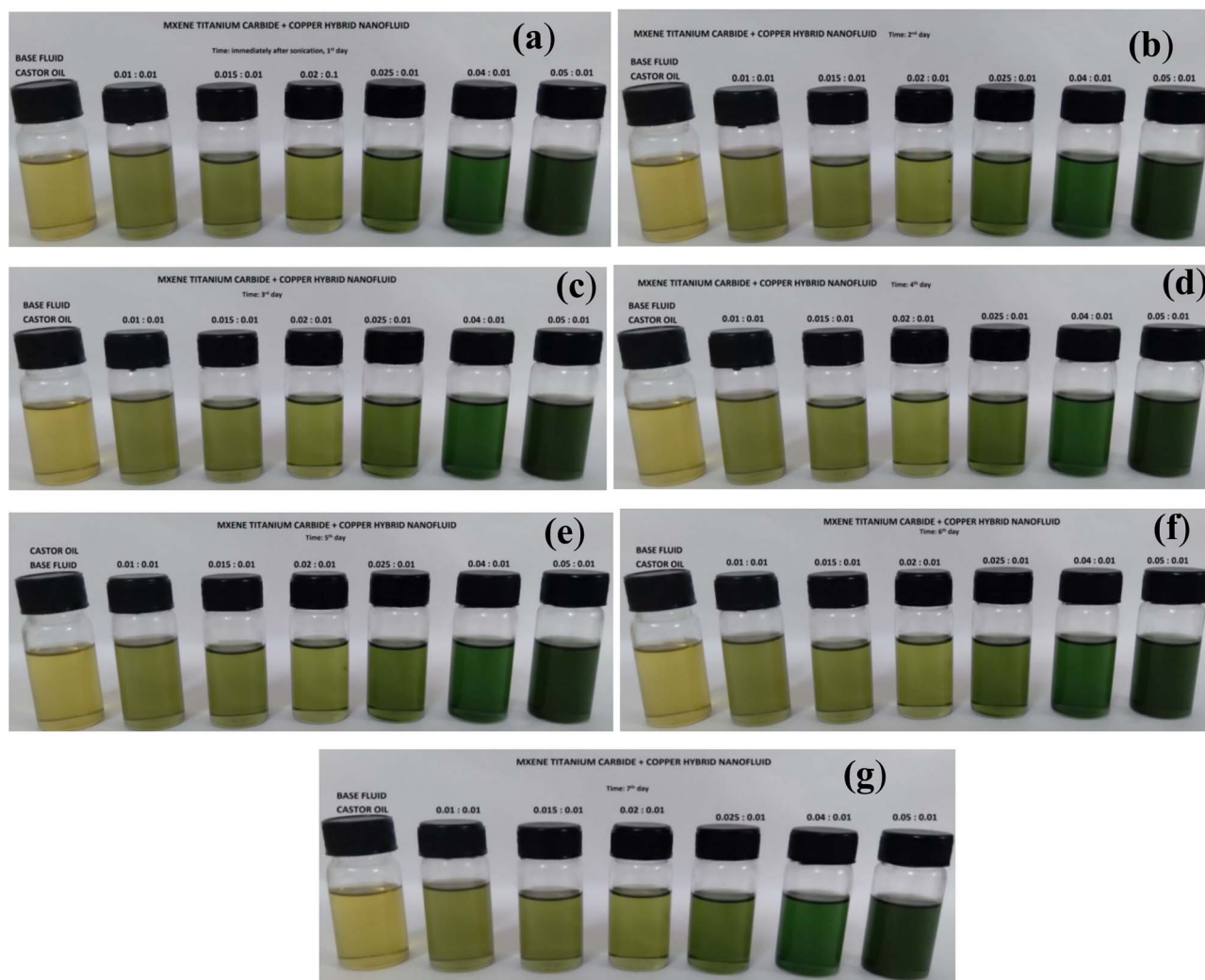
Fig. 11 Stability analysis of castor oil based Cu-MXene hybrid nanofluids through visual inspection: (a) after preparation (b) after 2 days (c) after 3 days (d) after 4 days (e) after 5 days (f) after 6 days (g) after 7 days.

as observed from the digital images where there is no significant notice of settled particles at the bottom of the vial.

Stability of Cu-MXene hybrid nanofluid synthesized using castor oil as base fluid is shown in Fig. 11. This hybrid nanofluid was prepared without adding surfactant. However, sonication time has been increased to 90 min in order to make sure that all Cu and MXene particles are clearly suspended in castor oil. After careful suspension of Cu and MXene particles in castor oil, stability of these castor oil based hybrid nanofluids was monitored visually with respect to time for at least 7 days and shown in Fig. 11. Castor oil based Cu-MXene hybrid nanofluid shown in Fig. 11 shows excellent stability against aggregation for a minimum of 7 days. This has been confirmed by the absence of sedimented Cu and MXene particles at the bottom of the vial with respect to time.

Silicone oil based Cu-MXene hybrid nanofluids stability was also captured visually with respect to time as shown in Fig. 12. These hybrid nanofluids also show excellent stability against aggregation even in the absence of surfactant. However, prolonged duration of sonication is provided to suspend the Cu

and MXene in silicone oil as similar to castor oil based hybrid nanofluids. Silicone oil based hybrid nanofluids displayed minimum 7 days of stability against settling of particles in the vial. This stability could be possibly due to the binding of siloxane group to the surface of Cu and MXene particles present in the silicone oil and thereby allowing the increase in repulsive forces among the particles.

In addition to visual interpretation of stability of mono and hybrid nanofluids, stability analysis was also further characterized using zeta potential measurements. Zeta potential analysis is a technique used to measure the stability of nanofluids by measuring the surface charge present on the surface of nanostructures. Higher the value of zeta potential, better will be the stability of nanofluids. Zeta potential of MXene and Cu-MXene nanofluids with respect to time is shown in Table 1.

3.3. Density of mono and hybrid nanofluids

Investigation of thermophysical properties such as density with respect to concentration of nanoparticles present in the base
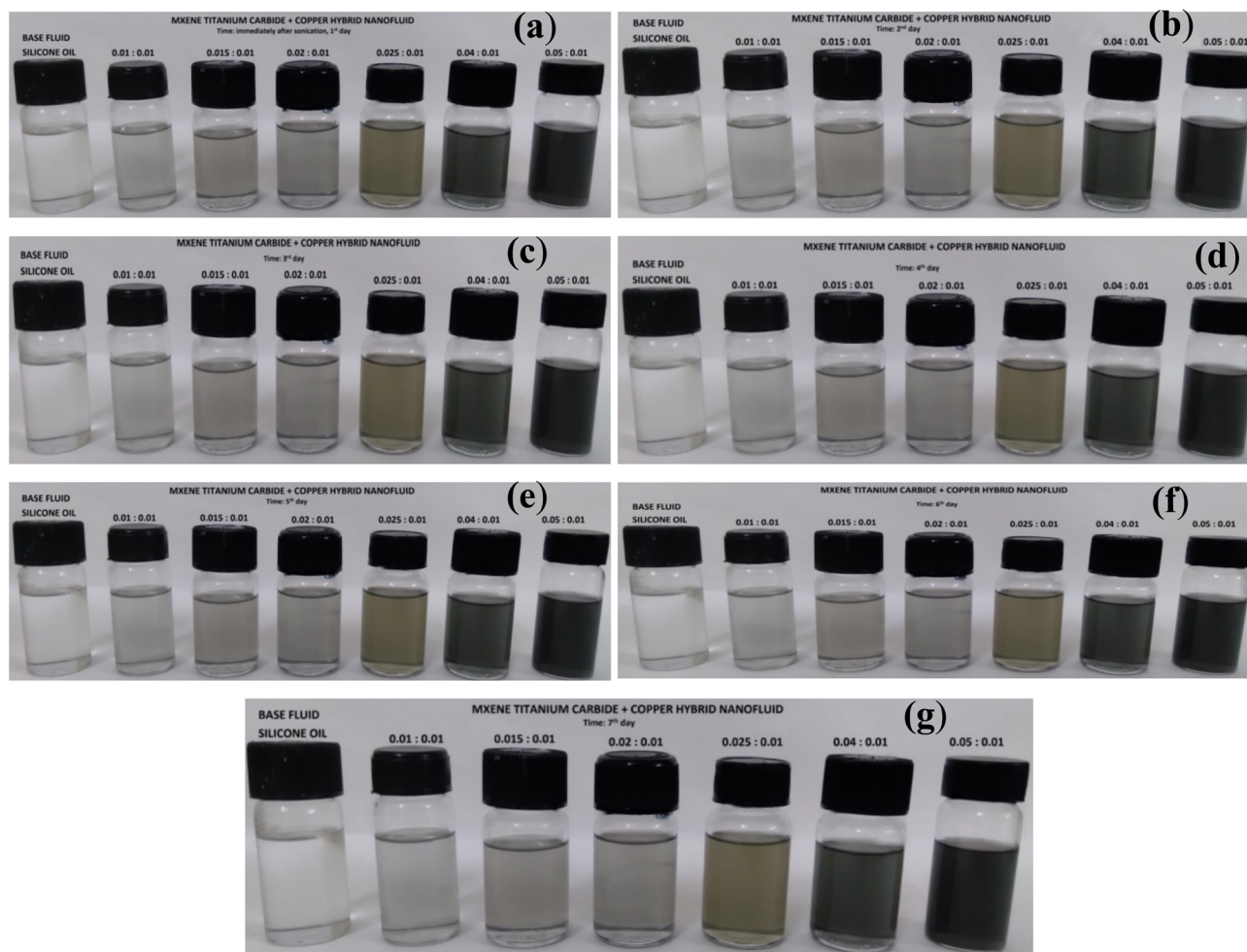
Fig. 12 Stability analysis of silicon oil based Cu-MXene hybrid nanofluids through visual inspection: (a) after preparation (b) after 2 days (c) after 3 days (d) after 4 days (e) after 5 days (f) after 6 days (g) after 7 days.

fluids is very essential for industrial heat transfer applications. Due to this reason, variation of mono and hybrid nanofluid density with respect to concentration of nanoparticles in different base fluids is studied and shown in Fig. 13. Since the pressure drop and pumping power is greatly influenced by density of fluid, effect of concentration of nanoparticles on density of the base fluid should be investigated thoroughly. From the Fig. 13, it can be seen that the density of the base fluids such as water, methanol, castor oil and silicone oil increases with increase in concentration of Cu, MXene and Cu-MXene nanoparticles. Similar trend was also reported by other researcher (Shoghl *et al.* (2016)).[42]

3.4. Wettability studies using contact angle measurement

One of the essential thermophysical properties of hybrid nanofluids is wetting. The degree of wetting of a fluid is determined by the contact angle. The contact angle (θ) is the angle formed by the tangent lines of the fluid droplet with the horizontal and level surface. Fluids possessing a contact angle greater than 90° are referred to as "hydrophobic" or "non-wetting" and the fluids showing a contact angle less than 90° is

referred as "hydrophilic" or "wetting".[27] The wettability of the prepared hybrid nanofluids in different base fluids are measured by measuring the contact angle and shown in Fig. 14. From the figure, it can be seen that the hybrid fluids synthesized using water, methanol, castor oil and silicone oil shows excellent wettability behavior as observed from the low contact angles which is less than 90° and also the contact angle decreases with increase in the concentration of MXene nanoparticles in base fluids. This could be possibly due to the larger size and higher density of Cu and MXene nanostructures as compared to liquid molecule which exerts excess downward force on the droplet allowing the contact angle to decrease with respect to increase in the concentration of nanostructures. Similar kind of behavior was also observed by Das *et al.* (2019).[43]

3.5. Thermal conductivity of mono and hybrid nanofluids

The most critical property for any nanofluid that needs to be considered for thermal applications is its thermal conductivity. Thermal conductivity of nanofluids plays a major role in enhancing the performance of heat exchangers during heating and cooling applications. Higher thermal conductivity

Table 1 Table representing the zeta potential of mono and hybrid nanofluids with respect to concentration of nanoparticles

S. no.	Type of nanofluid	MXene : Cu concentrations (vol%)	Zeta potential on day 0 (mV)	Zeta potential on day 7 (mV)
1	Water based MXene nanofluid	0.01 : 0	−46.8	−44.1
		0.015 : 0	−45.2	−43.6
		0.02 : 0	−44.9	−42.9
		0.025 : 0	−44.0	−41.7
		0.04 : 0	−43.1	−41.2
		0.05 : 0	−42.7	−40.3
2	Methanol based MXene nanofluid	0.01 : 0	−63.8	−61.7
		0.015 : 0	−62.1	−60.3
		0.02 : 0	−60.7	−58.6
		0.025 : 0	−59.2	−57.1
		0.04 : 0	−58.9	−56.5
		0.05 : 0	−58.6	−54.7
3	Water based Cu:MXene hybrid nanofluid	0.01 : 0.01	−43.5	−42.2
		0.015 : 0.01	−42.4	−41.5
		0.02 : 0.01	−41.1	−40.1
		0.025 : 0.01	−40.8	−39.6
		0.04 : 0.01	−40.2	−38.4
		0.05 : 0.01	−39.7	−37.8
4	Methanol based Cu:MXene hybrid nanofluid	0.01 : 0.01	−38.9	−37.3
		0.015 : 0.01	−38.2	−36.5
		0.02 : 0.01	−37.3	−35.9
		0.025 : 0.01	−36.1	−35.1
		0.04 : 0.01	−35.2	−34.2
		0.05 : 0.01	−34.4	−33.5

represents better enhancement in many heat transfer characteristics.[44] Fig. 15 shows the effect of concentration of MXene nanostructures on the thermal conductivity of MXene mono nanofluid and its enhancement as compared to different base fluids such as water, methanol, castor oil and silicone oil. From Fig. 15(a), it can be seen that the thermal conductivity of MXene mono nanofluid synthesized using water, methanol, castor oil and silicone oil base fluids increases with increase in the MXene particles loading. This incremental behavior in the thermal conductivity is possibly due to the high stability of nanofluid in all the base fluids at different particle concentrations as observed from the stability analysis. Further, enhancement in thermal conductivity was calculated based on thermal conductivity of base fluids and the nanofluids and shown in Fig. 15(b). It has been observed that the enhancement in thermal conductivity of all the nanofluids increases with increase in the concentration of MXene nanostructures in the base fluid. Methanol based MXene mono nanofluid represents higher enhancement (more than 50%) in thermal conductivity at higher particle loading (0.05 vol%) followed by castor oil based (more than 30%), water based (more than 15%) and silicone based (more than 8%) mono nanofluids.

Next, the experimental thermal conductivity values of MXene based nanofluids in different base fluids were compared with the existing theoretical models such as Maxwell and Hamilton Crosser model as shown in Fig. 16. Maxwell model was considered to be a first model which is applicable for low volume concentration of nanoparticles homogeneous suspensions.[44,45] It gives the relation between thermal conductivity of nanofluids as a function of thermal conductivity of nanoparticle, base fluid and concentration of nanoparticles as shown below.

$$k_{nf} = k_{bf} \left[\frac{k_{np} + 2k_{bf} + 2\varnothing_{np}(k_{np} - k_{bf})}{k_{np} + 2k_{bf} - \varnothing_{np}(k_{np} - k_{bf})} \right] \quad (1)$$

where, k_{nf}, k_{bf}, and k_{np} are the thermal conductivity of nanofluid, base fluid, nanostructure and $\varnothing_{np}$ represents the volume concentration of nanostructures.

Maxwell model was further modified by Hamilton and Crosser by incorporating the shape factor in the existing Maxwell model to study the effect of particle shape on the thermal conductivity of nanofluids as shown below[45]

$$k_{nf} = k_{bf} \left[\frac{k_{np} + (n-1)k_{bf} - (n-1)\,\varnothing_{np}(k_{bf} - k_{np})}{k_{np} + (n-1)k_{bf} + \varnothing_{np}(k_{bf} - k_n)} \right] \quad (2)$$

where, n is shape factor and is defined as $\frac{3}{\psi}$ and Ψ is the particle sphericity. From the Fig. 16, it can be observed that the water based MXene nanofluids alone fits with the experimental values of thermal conductivity. Whereas other MXene nanofluids synthesized using methanol, castor oil and silicon oil base fluids seems to under/over predict the effective thermal conductivity. This could be possibly due to the non-consideration of the effect of particle size and the interfacial layer at the particle–liquid interface in the conventional models listed above (Maxwell and Hamilton and Crosser). These effects play a major role in enhancing the thermal conductivity of nanofluids.

Next, we tried to further increase the thermal conductivity of all the base fluids by synthesizing hybrid nanofluids where two different nanostructures were added and dispersed in base fluid. Cu-MXene hybrid nanofluids were prepared by adding 0.01 vol% of Cu nanoparticles in addition to varied concentration of MXene nanoparticles (0.01, 0.015, 0.02, 0.025, 0.04 and 0.05 vol%) in base
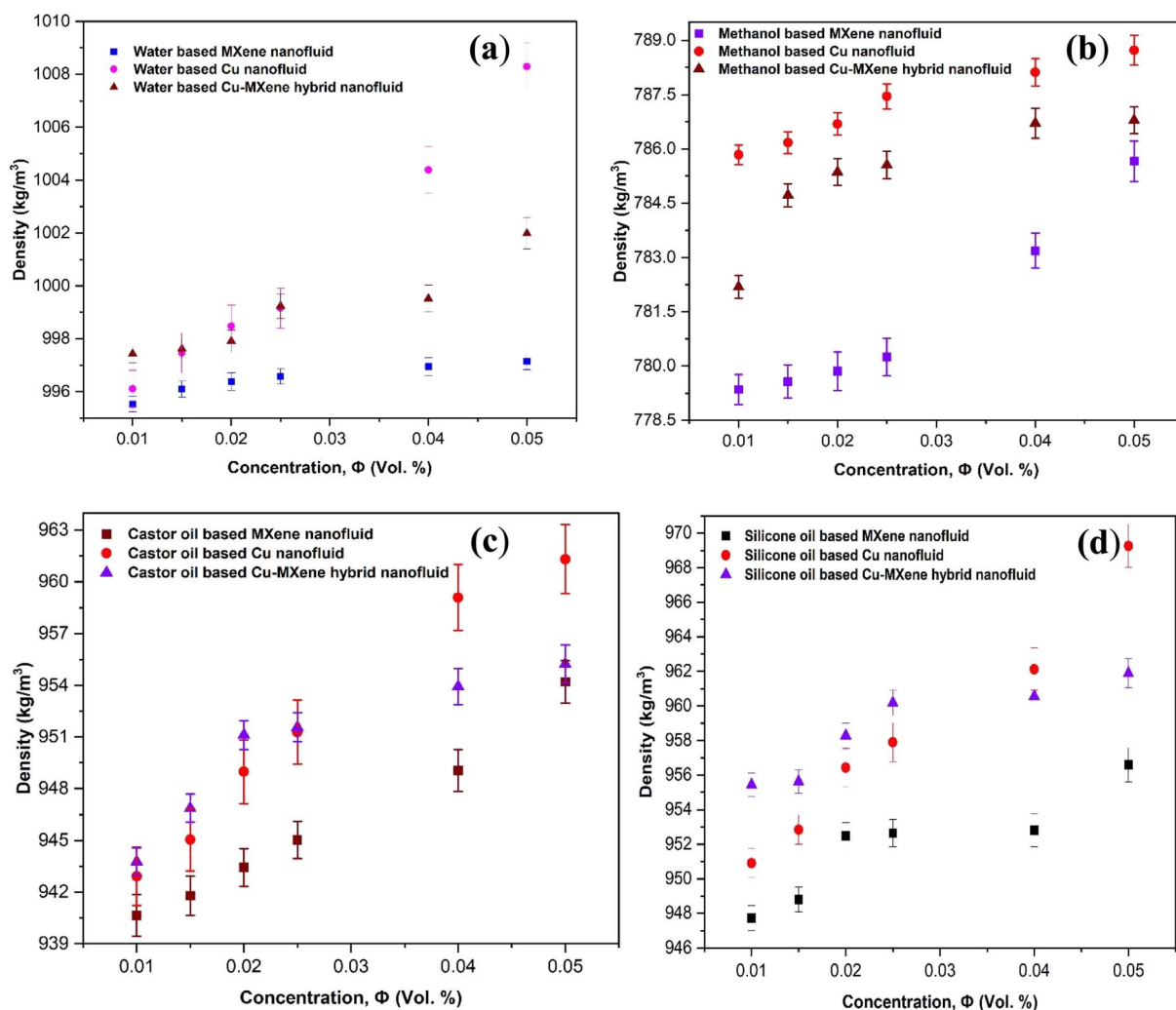
Fig. 13 Density of mono and hybrid nanofluids with respect to concentration of MXene nanoparticles in (a) water (b) castor oil (c) castor oil and (d) silicone oil.

fluids and thermal conductivity was measured successfully. Fig. 17(a) and (b) denotes the variation of thermal conductivity and enhancement of thermal conductivity with respect to increase in the concentration of MXene nanostructures by keeping Cu nanostructures concentration constant at 0.01 vol%. Form the figure, it can be seen that the thermal conductivity and enhancement in thermal conductivity increases with increase in the MXene particle loading in all the hybrid nanofluids due to strong behavior of stability. Moreover, a remarkable increase in the thermal enhancement of hybrid nanofluids (more than 70% in methanol, 40% in water and castor oil, and 10% in silicone oil)

noticed (shown in Fig. 17(b)) as compared to mono nanofluid shown in Fig. 15. This rise in enhancement of thermal conductivity may be possibly due to the collective effect of both Cu and MXene solid nanostructures in base fluids.

Cu-MXene based hybrid nanofluids experimental thermal conductivity values are also tried to validate with different existing conventional models such as modified Maxwell, Hamilton, and Yu and Choi models[45] as shown in Fig. 18. These models are applicable only for hybrid nanofluids and are shown below.

Modified Maxwell model:

$$k_{hnf} = k_{bf}\left[\frac{\frac{(\varnothing_{np1}k_{np1}+\varnothing_{np2}k_{np2})}{\varnothing}+2k_{bf}+2(\varnothing_{np1}k_{np1}+\varnothing_{np2}k_{np2})-2\varnothing k_{bf}}{\left(\frac{(\varnothing_{np1}k_{np1}+\varnothing_{np2}k_{np2})}{\varnothing}\right)+2k_{bf}-(\varnothing_{np1}k_{np1}+\varnothing_{np2}k_{np2})+\varnothing k_{bf}}\right] \quad (3)$$
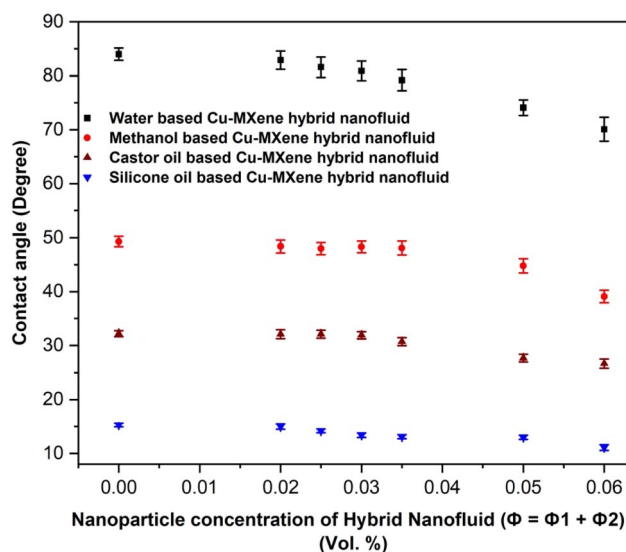
Fig. 14 Contact angle measurement with respect to volume concentration of Cu-MXene hybrid nanofluids prepared using different base fluids.

where, $\varnothing$ is the total volume concentration of nanostructures present in the hybrid mixture, $\varnothing_{np1}$ and $\varnothing_{np2}$ are the volume concentrations of nanoparticle 1 (copper) and nanoparticle 2 (MXene titanium carbide nanosheets). On the other hand, k_{hnf}, k_{bf}, k_{np1} and k_{np2} are the thermal conductivity of hybrid nanofluid, base fluid, nanoparticle 1 and nanoparticle 2 respectively.

Hamilton and Crosser model:

$$k_{hnf} = k_{bf} \left[\frac{k_{np1} + (n_1 - 1)k_{bf} - (n_1 - 1)\,\varnothing_{np1}(k_{bf} - k_{np1})}{k_{np1} + (n_1 - 1)k_{bf} + \varnothing_{np1}(k_{bf} - k_{np1})} \right]$$
$$\times \left[\frac{k_{np2} + (n_2 - 1)k_{bf} - (n_2 - 1)\varnothing_{np2}(k_{bf} - k_{np2})}{k_{np2} + (n_2 - 1)k_{bf} + \varnothing_{np2}(k_{bf} - k_{np2})} \right] \quad (4)$$

where n_1 and n_2 are the shape factor constituents of first and second particles respectively.

Yu and Choi model:

$$\frac{k_{hnf}}{k_{bf}} = \left(\frac{\left(k_{np2} + 2k_{bf} - 2\varnothing(k_{bf} - k_{np})(1 + \beta)^3\right)}{\left(k_{np2} + 2k_{bf} - \varnothing(k_{bf} - k_{np})(1 + \beta)^3\right)} \right) \quad (5)$$

where, β represents clustering effect.

After validating with these existing conventional models, it has been observed the water based hybrid nanofluids seems to fit best as compared to other base fluids based Cu-MXene hybrid nanofluids possibly due to the ignorance of other parameters (particle size, temperature, interfacial interactions etc.) in the models.

3.6. Specific heat of mono and hybrid nanofluids

Moreover, specific heat is another important thermophysical property for enhancing the thermal performance of heat transfer devices.[46,47] In this work, specific heat of mono nanofluids and hybrid nanofluids is calculated using the existing theoretical equations as shown below and the specific heat values with respect to concentration of nanoparticles are tabulated in Table 2.

For mono nanofluids,

$$C_{p,nf} = \left(\frac{\varnothing(\rho C_p)_n + (1 - \varnothing)(\rho C_p)_{bf}}{\varnothing\rho_n + (1 - \varnothing)\rho_{bf}} \right) \quad (6)$$

where $C_{p,nf}$, C_{pn}, C_{pbf} are specific heat of mono nanofluid, nanoparticle and base fluid respectively and ρ_n, ρ_{bf} represents density of nanoparticle and base fluid. Finally, the concentration of nanoparticles was denoted by $\varnothing$.

For hybrid nanofluids,

$$(\rho C_p)_{hnf} = \varnothing_1(\rho C_p)_{s1} + \varnothing_2(\rho C_p)_{s2} + (1 - \varnothing)(\rho C_p)_f \quad (7)$$

where, C_{phnf}, C_{ps1}, C_{ps2}, C_{pf} shows the specific heat of hybrid nanofluid, nanoparticle 1, nanoparticle 2 and base fluid. ρ_{hnf},
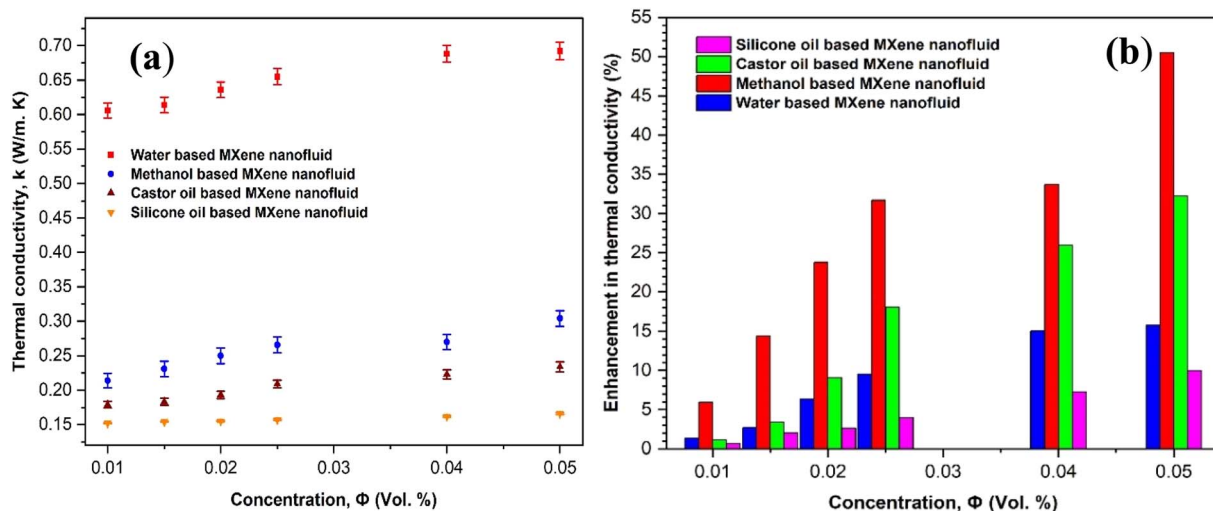

Fig. 15 Effect of concentration of MXene nanostructures on (a) thermal conductivity and (b) the enhancement of thermal conductivity in different base fluid centered MXene mono nanofluids.
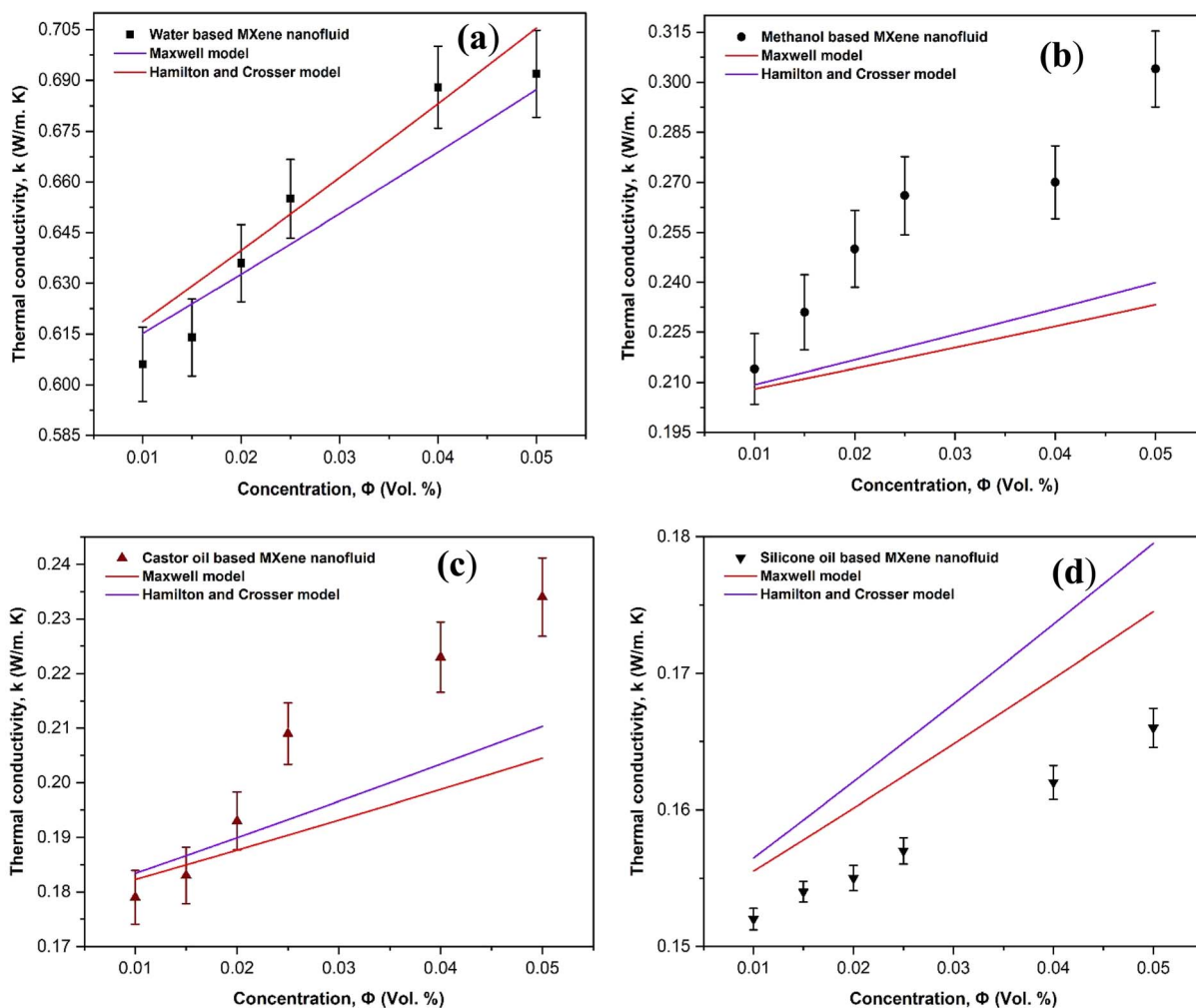
Fig. 16 Validation of experimental thermal conductivity with the existing model equations for (a) water based (b) methanol based (c) castor oil based and (d) silicon oil based MXene mono nanofluids.
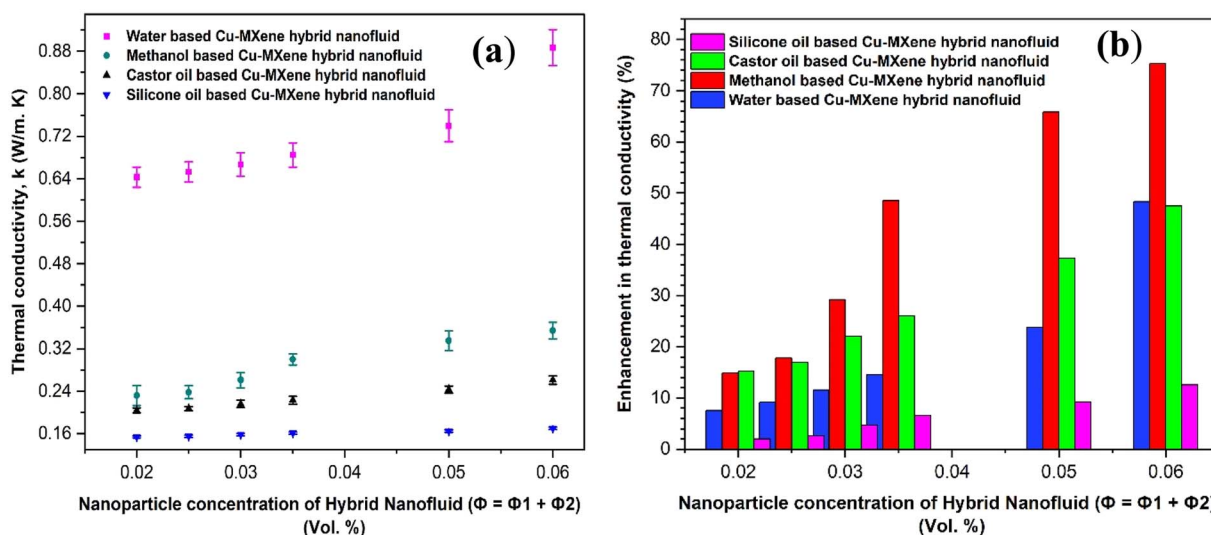

Fig. 17 Effect of concentration of MXene nanostructures on (a) thermal conductivity of base fluids and (b) the enhancement of thermal conductivity in hybrid nanofluids.
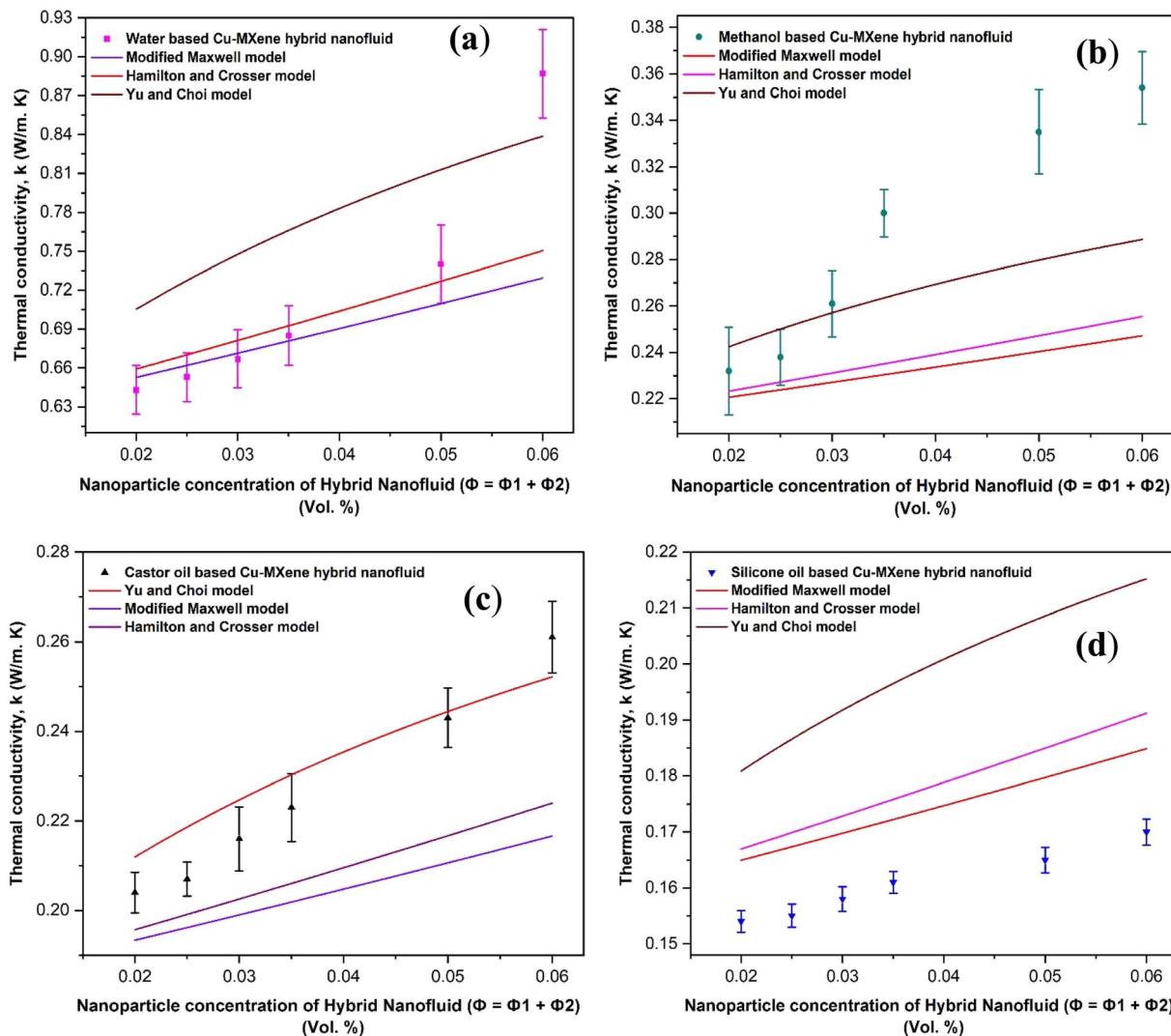
Fig. 18 Validation of experimental thermal conductivity with the existing model equations for (a) water (b) methanol (c) castor oil and (d) silicon oil based Cu-MXene hybrid nanofluids.

ρ_{s1}, ρ_{s2} and ρ_f represents the density of hybrid nanofluid, nanoparticle 1, nanoparticle 2 and base fluid respectively. $\varnothing, \varnothing_1$ and $\varnothing_2$ denotes the total volume concentration and volume concentration of nanoparticle 1 and nanoparticle 2.

From Table 2, it has been observed that the specific heat of MXene mono and Cu-MXene hybrid nanofluids synthesized using water, methanol, castor oil and silicone oil as base fluids decreases with increase in the concentration of MXene/Cu-MXene nanoparticles which could be due to the availability of less energy with respect to increase in the concentration of nanoparticles for activating the nanoparticles. In addition, solid particles will have less specific heat as compared to liquids which in turn collectively reduces the specific heat of mono/hybrid nanofluids by adding the solid nanoparticles in base fluids. Hence it has confirmed that different base fluids and the presence of more than one nanostructure influence the specific heat of nanofluids.

3.7. Viscosity of mono and hybrid nanofluids

The rheological behavior of the synthesized hybrid nanofluids using different base fluids was measured at room temperature and shown in Fig. 19(a) and (b). Viscosity of hybrid nanofluids increases with increase in the concentration of MXene nanostructures in the base fluid which is due to the increase in van der Waals force of attraction between base fluids and the solid MXene nanostructures. Thereby, hybrid nanofluid viscosity increases remarkably as compared to base fluids viscosity as shown in Fig. 19(a) and (b). Approximately, 85% enhancement in viscosity of the water and methanol based hybrid nanofluid has been reported as compared to the base fluids such as water and methanol. However, a slight enhancement (∼11%) in the viscosity of castor oil based hybrid nanofluids was observed as compared to castor oil base fluid. A massive enhancement in viscosity of silicone based hybrid nanofluids (∼340%) has been noticed as compared to silicone oil base fluid viscosity

Table 2 Table representing the specific heat mono and hybrid nanofluids with respect to concentration of nanoparticles

S. no.	Type of nanofluid	Concentration of MXene/Cu-MXene nanoparticles (vol%)	Specific heat ($J\ kg^{-1}\ K^{-1}$)
1	Water based MXene nanofluid	0.01	4036.69
		0.015	3967.87
		0.02	3901.14
		0.025	3836.4
		0.04	3653.28
		0.05	3539.69
2	Methanol based MXene nanofluid	0.01	2404.55
		0.015	2359.78
		0.02	2316.83
		0.025	2275.59
		0.04	2161.13
		0.05	2091.72
3	Castor oil based MXene nanofluid	0.01	1672.976
		0.015	1642.293
		0.02	1612.636
		0.025	1583.958
		0.04	1503.381
		0.05	1453.832
4	Silicone oil based MXene nanofluid	0.01	1157.42
		0.015	1146.69
		0.02	1136.3
		0.025	1126.25
		0.04	1097.94
		0.05	1080.47
5	Water based Cu-MXene hybrid nanofluid	0.02	3695.637
		0.025	3627.494
		0.03	3561.368
		0.035	3497.176
		0.05	3315.409
		0.06	3202.543
6	Methanol based Cu-MXene hybrid nanofluid	0.02	2142.934
		0.025	2095.174
		0.03	2049.304
		0.035	2005.217
		0.05	1882.748
		0.06	1808.444
7	Castor oil based Cu-MXene hybrid nanofluid	0.02	1672.976
		0.025	1642.293
		0.03	1612.636
		0.035	1583.958
		0.05	1503.381
		0.06	1453.832
8	Silicone oil based Cu-MXene hybrid nanofluid	0.02	1042.879
		0.025	1025.031
		0.03	1007.821
		0.035	991.219
		0.05	944.804
		0.06	916.451

suggesting the extraordinary interaction between silicone oil base fluid and the MXene nanostructures.

Viscosity of hybrid nanofluids measured using viscometer with respect to variation in the concentration of nanoparticles were tried to validate with the existing theoretical model equations as shown in Fig. 20. Six model equations such as Park and Cho, Brinkman, Einstein, Sharma, Chen *et al.* and Batchelor models[48] were identified which are represented as viscosity of hybrid nanofluids as a function of viscosity of base fluids and concentration of nanoparticles as shown below.

Pak and Cho model:

$$\mu_{hnf} = \mu_{bf}(1 + 39.11 \times \varnothing + 533.9 \times \varnothing^2) \quad (8)$$

Brinkman model:

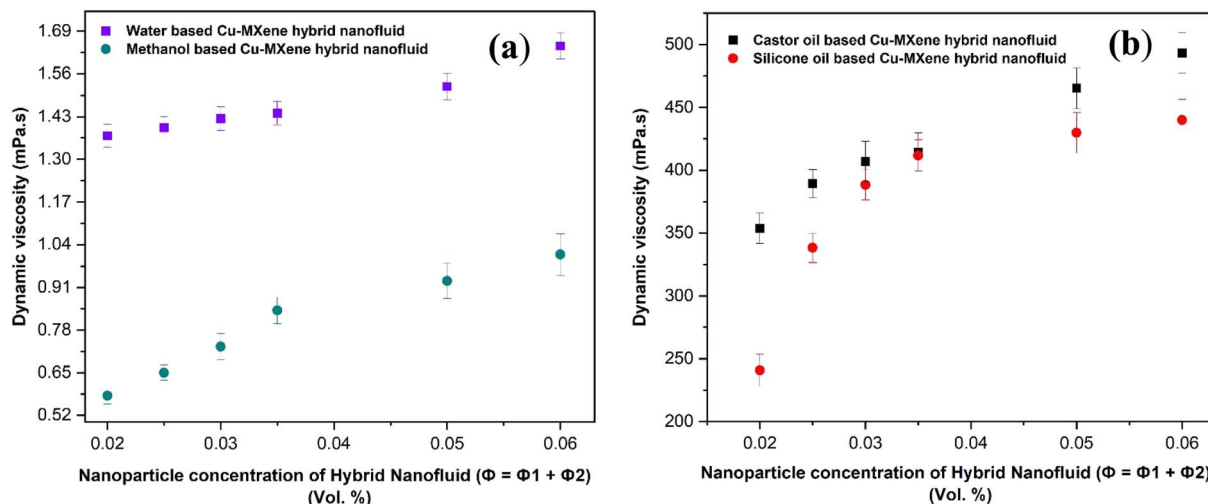$$\mu_{hnf} = \mu_{bf}\left(\frac{1}{(1 - \varnothing)^2}\right) \quad (9)$$

Fig. 19 Effect of concentration of MXene nanostructures on viscosity of (a) water, methanol based and (b) castor oil, silicone oil based Cu–MXene hybrid nanofluids.
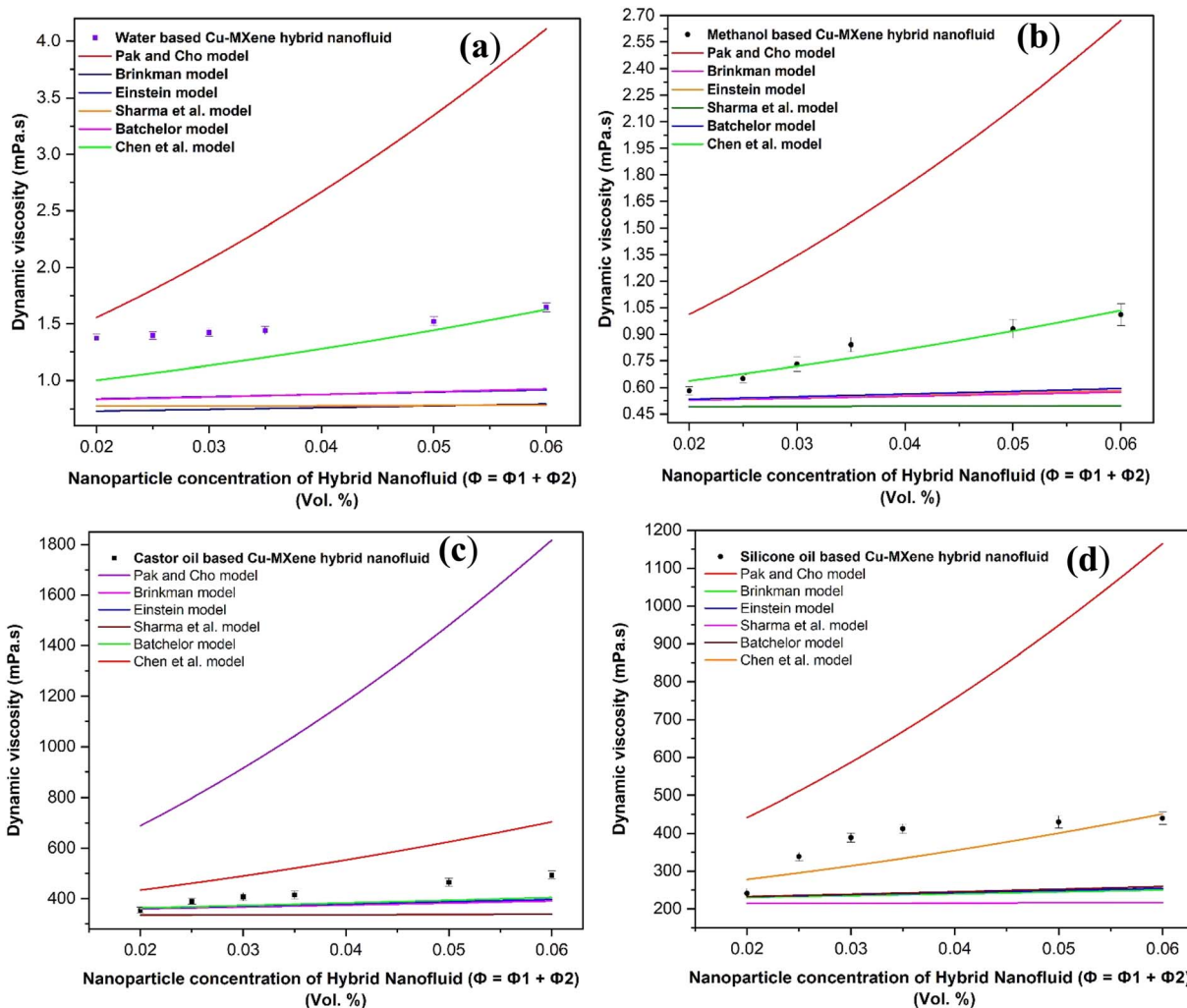

Fig. 20 Validation of experimental viscosity data with the existing model equations for (a) water (b) methanol (c) castor oil and (d) silicon oil based Cu–MXene hybrid nanofluids.

Table 3   Table representing the pumping power of hybrid nanofluids with respect to concentration of nanoparticles

S. no.	Type of nanofluid	Concentration of MXene/Cu-MXene nanoparticles (vol%)	Pumping power (W)
1	Water based Cu-MXene hybrid nanofluid	0.02	5.013
		0.025	5.012
		0.03	5.011
		0.035	5.004
		0.05	5.002
		0.06	4.990
2	Methanol based Cu-MXene hybrid nanofluid	0.02	6.392
		0.025	6.372
		0.03	6.366
		0.035	6.365
		0.05	6.356
		0.06	6.355
3	Castor oil based Cu-MXene hybrid nanofluid	0.02	5.298
		0.025	5.281
		0.03	5.257
		0.035	5.254
		0.05	5.241
		0.06	5.234
4	Silicone oil based Cu-MXene hybrid nanofluid	0.02	5.233
		0.025	5.232
		0.03	5.218
		0.035	5.207
		0.05	5.205
		0.06	5.198

Einstein viscosity correlation:

$$\mu_{hnf} = \mu_{bf}(1 + 2.5 \times \varnothing \qquad (10)$$

Sharma et al. model:

$$\mu_{hnf} = \mu_{bf}\left(0.9653 + 77.4567\left(\frac{\varnothing_{hnf}}{100}\right)^{1.1558}\left(\frac{T_1}{T_2}\right)^{0.6801}\right) \qquad (11)$$

Chen et al. viscosity model:

$$\mu_{nf} = \mu_{bf}(1 + 10.6 \times \varnothing + (10.6 \times \varnothing)^2) \qquad (12)$$

Batchelor model:

$$\mu_{nf} = \mu_{bf}(1 + 2.5 \times \varnothing + 6.2 \times \varnothing^2) \qquad (13)$$

where: μ_{hnf} and μ_{bf} are viscosities of hybrid and base fluids and $\varnothing$ is the total volume concentration of nanoparticles. T_1 and T_2
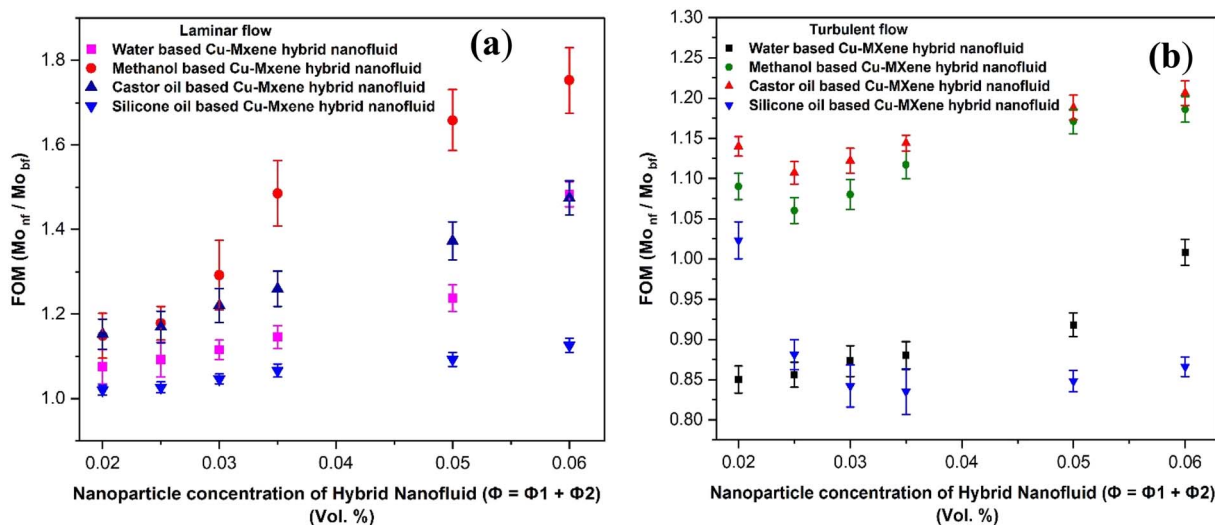

Fig. 21   FOM analysis of CU-MXene hybrid nanofluids under (a) laminar and (b) turbulent flow conditions.

represent initial and final temperature of the hybrid nanofluid respectively. From Fig. 20, it can be seen that the Chen *et al.* model fitted well with the water, methanol and silicone oil based hybrid nanofluids. On the other hand, castor oil based hybrid nanofluids fitted with Batchelor model instead of Chen *et al.* model.

3.8. Pumping power of hybrid nanofluids

Pumping power is one of the important parameters which decide the economical performance of any heat exchanging device. In this paper, pumping power of hybrid nanofluids were calculated using the following equation by assuming the parameters like mass flow rate (0.1 kg s^{-1}) and pressure drop (0.5×10^5 Pa) and tabulated in Table 3. From the Table 3, it has been observed that the hybrid nanofluids exhibits low pumping power ranging from 5–6 W which signifies lower energy consumption in transporting the hybrid nanofluids in heat exchanging devices.

$$\text{Pumping power} = \left(\frac{m}{\rho_{\text{hnf}}}\right) \times \Delta P \qquad (14)$$

where m, ρ_{hnf}, and ΔP represents mass flow rate, density and pressure drop of hybrid nanofluids respectively.

3.9. Figure of merit (FOM) analysis

The thermal effectiveness of any heat transfer fluid was measured using a dimensionless number known as Mouromtseff number (Mo). Mouromtseff number was first introduced by Simons[49] to examine the thermal effectiveness of heat transfer fluid for electronic cooling application. Mouromtseff number is considered as a Figure of merit for discussing the thermal performance of heat transfer fluids. Higher the Mouromtseff number better will be the thermal performance of any coolant.[28] For fully developed internal laminar and turbulent flow, the Mouromtseff number can be estimated using the following expression.

FOM under laminar and turbulent flow regimes [28] can be calculated as follows:

$$\text{FOM}_{\text{laminar}} = \frac{k_{\text{nf}}}{k_{\text{bf}}} = \frac{(\mu_{\text{nf}} - \mu_{\text{bf}})}{k_{\text{nf}} - k_{\text{bf}}} \qquad (15)$$

$$\text{FOM}_{\text{turbulent}} = \frac{\text{Mo}_{\text{nf}}}{\text{Mo}_{\text{bf}}}$$
$$= \left(\frac{k_{\text{nf}}}{k_{\text{bf}}}\right)^{0.6} \times \left(\frac{\rho_{\text{nf}}}{\rho_{\text{bf}}}\right)^{0.8} \times \left(\frac{c_{\text{pnf}}}{c_{\text{pbf}}}\right)^{0.4} \times \left(\frac{\mu_{\text{nf}}}{\mu_{\text{bf}}}\right)^{-0.47} \qquad (16)$$

$$\text{where, } \text{Mo} = \left(\frac{\rho^a k^b C_p{}^d}{\mu^e}\right) \qquad (17)$$

where Mo_{nf}, Mo_{bf}, k_{nf} and k_{bf}, ρ_{nf}, ρ_{bf}, μ_{nf}, μ_{bf}, c_{pnf} and c_{pbf} represents Mouromtseff number, thermal conductivity, density, dynamic viscosity, and specific heat of the nanofluid and base fluid respectively and $a = 0.8$, $b = 0.6$, $d = 0.4$, and $e = 0.47$ as reported by Said *et al.* (2022).[50] FOM value greater than 1 suggests that it can be considered as a favorable for that

Table 4 A comparative table between the current work and existing literature

Ref.	Nanoparticles	Concentration	Base fluid	Synthesis method	Dispersant	Enhancement in thermophysical property (%)		FOM analysis conducted (yes/no)
						Viscosity	Thermal conductivity	
Suresh *et al.*[12]	Al$_2$O$_3$–Cu	0.1 to 2 vol%	Water	Two-step method	SLS	78	12.11	No
Abbasi *et al.*[13]	γAl$_2$O$_3$-MWCNT	0.2 to 1 vol%	Water	Two-step method	GA	—	14.7	No
Esfe *et al.*[19]	Graphene	0.1 to 2 mass%	Water	Two-step method	PVP	45	96	No
Mostafizur *et al.*[23]	Al$_2$O$_3$-MWCNT	0.1 to 0.5 vol%	Radiator coolant	Two-step method	SDS	11	13.7	Yes (FOM >1)
Mane *et al.*[28]	CuO–Fe$_3$O$_4$	0.1 wt%	Water	Two-step method	Chitosan	10	4.9	Yes (FOM >1)
Chen *et al.*[41]	CuO, MgO, CNT, TiO$_2$, Al$_2$O$_3$ and ZnO	0.01 to 2 wt%	Water	Two-step method	SDS	1	No	No
Our work	Cu-MXene	0.02 to 0.06 vol%	Water, methanol, castor oil, and silicone oil	Two-step method	SDS	10–340	10–70	Yes

particular region (laminar or turbulent). FOM under fully developed laminar and turbulent flow condition was evaluated using the thermal conductivity, density, specific heat and viscosity of nanofluid, base fluid for Cu-MXene hybrid nanofluid with respect to concentration of particles and shown in Fig. 21. From Fig. 21(a), it can be observed that Cu-MXene hybrid nanofluids represents larger FOM value which is greater than 1 under laminar flow conditions for all the samples signifying better heat transfer capability under fully developed laminar flow conditions. The phenomena is not same for water and silicone oil based Cu-MXene hybrid nanofluids under turbulent flow conditions as observed from the smaller value of FOM (less than 1) in Fig. 21(b) indicating its non-suitability for enhancing the heat transfer performance under turbulent flow conditions. However, methanol and castor oil based Cu-MXene hybrid nanofluids hold FOM value greater than 1 under turbulent flow.

Finally, a comparative study has been performed by comparing our work with already published works in terms of concentration of nanostructures, thermo-physical properties, FOM analysis conducted and shown in Table 4. From this analysis, it has been observed that MXene mono and Cu-MXene hybrid nanofluids synthesized in the current work display remarkable enhancement in thermophysical properties at low concentration of nanostructures as compared to other material based nanofluids reported in the literature.

3.10. Uncertainty analysis

ASTM Test Code PTC 19.8 has been used to perform the uncertainty analysis.[51] All the measurements conducted for computing various thermo-physical properties such as density, thermal conductivity, contact angle and viscosity are repeated for at least 3 times to achieve the consistency and reliability in the data. Finally, the mean data is reported by considering the standard error value. The percentage error data calculated for density, thermal conductivity, contact angle and viscosity is found to be 1%, 6%, 4% and 2% respectively. Uncertainty analysis is ignored for other properties such as specific heat and pumping as they are computed theoretically using existing correlations.

4 Conclusion

Cu and MXene nanostructures required for preparing mono and hybrid nanofluids were successfully synthesized using chemical reduction and HF etching methods. Cu nanoparticles represents the average particle size of ~20 nm and MXene nanostructures shows a layered structure as observed from TEM and FESEM analysis. Mono and hybrid nanofluids were effectively prepared using two step method by dispersing the low concentration Cu and MXene nanostructures in various base fluids. As prepared mono and hybrid nanofluids shows excellent stability against aggregation in all the base fluids.

Thermo-physical properties such as density, thermal conductivity, viscosity and wettability of hybrid nanofluids were successfully measured and reported a maximum enhancement

in thermal conductivity and viscosity of nanofluids at very low concentration of nanostructures. In addition, specific heat and pumping power of hybrid nanofluids were also determined using theoretical equations obtained from the literature and observed that these properties decreases with increase in the volume concentration of nanostructures. Experimental thermal conductivity and viscosity of hybrid nanofluids were also successfully validated with the well-known existing theoretical correlations. Finally, better heat transfer fluid was suggested enhancing the thermal performance of heat exchanging devices under laminar and turbulent flow conditions by conducting the FOM analysis.

Conflicts of interest

Authors declare no conflict of interest.

References

1 L. Das, K. Habib, K. Irshad, R. Saidur, S. Algarni and T. Alqahtani, Thermo-Optical Characterization of Therminol55 Based MXene–Al$_2$O$_3$ Hybridized Nanofluid and New Correlations for Thermal Properties, *Nanomaterials*, 2022, **12**, 1862, DOI: 10.3390/nano12111862.

2 J. P. Vallejo, G. Żyła, L. Ansia, J. Fal, J. Traciak and L. Lugo, Thermophysical, rheological and electrical properties of mono and hybrid TiB$_2$/B$_4$C nanofluids based on a propylene glycol:water mixture, *Powder Technol.*, 2022, **395**, 391–399, DOI: 10.1016/j.powtec.2021.09.074.

3 S. U. S. Choi, Nanofluids: From Vision to Reality Through Research, *J. Heat Transfer*, 2009, **131**, 033106, DOI: 10.1115/1.3056479.

4 I. Gonçalves, R. Souza, G. Coutinho, J. Miranda, A. Moita, J. E. Pereira, A. Moreira and R. Lima, Thermal conductivity of nanofluids: A review on prediction models, controversies and challenges, *Appl. Sci.*, 2021, **11**, 2525, DOI: 10.3390/app11062525.

5 J. Dong, Q. Zheng, C. Xiong, E. Sun and J. Chen, Experimental investigation and application of stability and thermal characteristics of SiO$_2$-ethylene-glycol/water nanofluids, *Int. J. Therm. Sci.*, 2022, **176**, 107533, DOI: 10.1016/j.ijthermalsci.2022.107533.

6 W. V. Vicki, M. Z. Abdullah and P. Gunnasegaran, Effect of volume concentration and nanofluid temperature on the thermal conductivity of mono and hybrid Al$_2$O$_3$-TiO$_2$ nanofluid, *AIP Conf. Proc.*, 2021, **2339**, 020079, DOI: 10.1063/5.0044204.

7 J. A. Ranga Babu, K. K. Kumar and S. Srinivasa Rao, State-of-art review on hybrid nanofluids, *Renewable Sustainable Energy Rev.*, 2017, **77**, 551–565, DOI: 10.1016/j.rser.2017.04.040.

8 X. Ma, L. Yang, G. Xu and J. Song, A comprehensive review of MXene-based nanofluids: Preparation, stability, physical properties, and applications, *J. Mol. Liq.*, 2022, **365**, 120037, DOI: **10.1016/j.molliq.2022.120037**.

9 S. Chakraborty and P. K. Panigrahi, Stability of nanofluid: A review, *Appl. Therm. Eng.*, 2020, **174**, 115259, DOI: **10.1016/j.applthermaleng.2020.115259**.

10 R. Azizian, E. Doroodchi and B. Moghtaderi, Effect of nanoconvection caused by Brownian motion on the enhancement of thermal conductivity in nanofluids, *Ind. Eng. Chem. Res.*, 2012, **51**, 1782–1789, DOI: **10.1021/ie201110k**.

11 M. U. Sajid and H. M. Ali, Thermal conductivity of hybrid nanofluids: A critical review, *Int. J. Heat Mass Transfer*, 2018, **126**, 211–234, DOI: **10.1016/j.ijheatmasstransfer.2018.05.021**.

12 S. Suresh, K. P. Venkitaraj, P. Selvakumar and M. Chandrasekar, Synthesis of Al_2O_3-Cu/water hybrid nanofluids using two step method and its thermo physical properties, *Colloids Surf., A*, 2011, **388**, 41–48, DOI: **10.1016/j.colsurfa.2011.08.005**.

13 S. M. Abbasi, A. Rashidi, A. Nemati and K. Arzani, The effect of functionalisation method on the stability and the thermal conductivity of nanofluid hybrids of carbon nanotubes/gamma alumina, *Ceram. Int.*, 2013, **39**, 3885–3891, DOI: **10.1016/j.ceramint.2012.10.232**.

14 T. T. Baby and R. Sundara, Synthesis of silver nanoparticle decorated multiwalled carbon nanotubes-graphene mixture and its heat transfer studies in nanofluid, *AIP Adv.*, 2013, **3**, 012111, DOI: **10.1063/1.4789404**.

15 M. J. Nine, M. Batmunkh, J. H. Kim, H. S. Chung and H. M. Jeong, Investigation of Al_2O_3-MWCNTs hybrid dispersion in water and their thermal characterization, *J. Nanosci. Nanotechnol.*, 2012, **12**(6), 4553–4559, DOI: **10.1166/jnn.2012.6193**.

16 T. P. Teng and Y. H. Hung, Estimation and experimental study of the density and specific heat for alumina nanofluid, *J. Exp. Nanosci.*, 2014, **9**, 707–718, DOI: **10.1080/17458080.2012.696219**.

17 H. Babar, M. U. Sajid and H. M. Ali, Viscosity of hybrid nanofluids: A Critical Review, *Therm. Sci.*, 2019, **23**, 1713–1754, DOI: **10.2298/TSCI181128015B**.

18 M. Hemmat Esfe, S. Alidoust, E. Mohammadnejad Ardeshiri, M. H. Kamyab and D. Toghraie, Experimental Study of Rheological Behavior of MWCNT-Al_2O_3/SAE50 Hybrid Nanofluid to Provide the Best Nano-lubrication Conditions, *Nanoscale Res. Lett.*, 2022, **17**, 4, DOI: **s11671-021-03639-3**.

19 M. H. Esfe, S. Esfandeh, M. H. Kamyab and D. Toghraie, Analysis of rheological behavior of MWCNT-Al_2O_3 (10:90)/5W50 hybrid non-Newtonian nanofluid with considering viscosity as a three-variable function, *J. Mol. Liq.*, 2021, **341**, 117375, DOI: **10.1016/j.molliq.2021.117375**.

20 V. Wanatasanappan, P. Kumar Kanti, P. Sharma, N. Husna and M. Z. Abdullah, Viscosity and rheological behavior of Al_2O_3-Fe_2O_3/water-EG based hybrid nanofluid: A new correlation based on mixture ratio, *J. Mol. Liq.*, 2023, **375**, 121365, DOI: **10.1016/j.molliq.2023.121365**.

21 G. Huminic, A. Huminic, C. Fleacă, F. Dumitrache and I. Morjan, Experimental study on viscosity of water based Fe–Si hybrid nanofluids, *J. Mol. Liq.*, 2021, **321**, 114938, DOI: **10.1016/j.molliq.2020.114938**.

22 S. U. Ilyas, R. Shamsuddin, T. Kai Xiang, P. Estellé and R. Pendyala, Rheological profile of graphene-based nanofluids in thermal oil with hybrid additives of carbon nanotubes and nanofibers, *J. Mol. Liq.*, 2023, **376**, 121443, DOI: **10.1016/j.molliq.2023.121443**.

23 R. M. Mostafizur, M. G. Rasul, M. N. Nabi and G. Saianand, Properties of Al_2O_3-MWCNT/radiator coolant hybrid nanofluid for solar energy applications, *Energy Rep.*, 2022, **8**, 582–591, DOI: **10.1016/j.egyr.2022.10.240**.

24 G. Huminic and A. Huminic, Heat transfer capability of the hybrid nanofluids for heat transfer applications, *J. Mol. Liq.*, 2018, **272**, 857–870, DOI: **10.1016/j.molliq.2018.10.095**.

25 S. Chakraborty, I. Sarkar, D. K. Behera, S. K. Pal and S. Chakraborty, Experimental investigation on the effect of dispersant addition on thermal and rheological characteristics of TiO_2 nanofluid, *Powder Technol.*, 2017, **307**, 10–24, DOI: **10.1016/j.powtec.2016.11.016**.

26 E. B. Elcioglu, A. M. Genc, Z. H. Karadeniz, M. A. Ezan and A. Turgut, Nanofluid figure-of-merits to assess thermal efficiency of a flat plate solar collector, *Energy Convers. Manage.*, 2020, **204**, 112292, DOI: **10.1016/j.enconman.2019.112292**.

27 A. Marmur, C. Della Volpe, S. Siboni, A. Amirfazli and J. W. Drelich, Contact angles and wettability: Towards common and accurate terminology, *Surf. Innovations*, 2017, **5**, 3–8, DOI: **10.1680/jsuin.17.00002**.

28 N. S. Mane, S. Tripathi and V. Hemadri, Effect of biopolymers on stability and properties of aqueous hybrid metal oxide nanofluids in thermal applications, *Colloids Surf., A*, 2022, **643**, 128777, DOI: **10.1016/j.colsurfa.2022.128777**.

29 X. Ma, Y. Song, Y. Wang, Y. Zhang, J. Xu, S. Yao and K. Vafai, Experimental study of boiling heat transfer for a novel type of GNP-Fe_3O_4 hybrid nanofluids blended with different nanoparticles, *Powder Technol.*, 2022, **396**, 92–112, DOI: **10.1016/j.powtec.2021.10.029**.

30 P. Mahajan, S. Verma, B. Padha, A. Ahmed and S. Arya, Manganese oxide and nickel oxide thin films on polyester to enable self-charging wearable supercapacitor, *J. Alloys Compd.*, 2023, **968**, 171904, DOI: **10.1016/j.jallcom.2023.171904**.

31 S. Verma, P. Mahajan, B. Padha, A. Ahmed and S. Arya, Nanowires based solid-state asymmetric self-charging supercapacitor driven by PVA–ZnO–KOH flexible piezoelectric matrix, *Electrochim. Acta*, 2023, **465**, 142933, DOI: **10.1016/j.electacta.2023.142933**.

32 M. Singh, W. U. Haq, S. Bishnoi, B. P. Singh, S. Arya, A. Khosla and V. Gupta, Investigating photoluminescence properties of Eu^{3+} doped $CaWO_4$ nanoparticles via Bi^{3+} amalgamation for w-LEDs application, *Mater. Technol.*, 2022, **37**, 1051–1061, DOI: **10.1080/10667857.2021.1918866**.

33 D. K. Bal, M. R. Chandan, R. Taneja, R. R. Tiwari, S. Saboor, D. Mishra, A. Ghosh and A. H. Shaik, Biocompatible polymer-capped oxidation-resistant copper nanoparticles for nanofluid and hydrogel applications, *Eur. Phys. J. Plus*, 2022, **137**, 1–16, DOI: **10.1140/epjp/s13360-021-02280-4**.

34 E. A. Kumar, T. Kokulnathan, T. J. Wang, A. J. Anthuvan and Y. H. Chang, Two-dimensional titanium carbide (MXene) nanosheets as an efficient electrocatalyst for 4-nitroquinoline N-oxide detection, *J. Mol. Liq.*, 2020, **312**, 113354, DOI: **10.1016/j.molliq.2020.113354**.

35 P. P. Chowdhury, A. H. Shaik and J. Chakraborty, Preparation of stable sub 10 nm copper nanopowders redispersible in polar and non-polar solvents, *Colloids Surf., A*, 2015, **466**, 189–196, DOI: **10.1016/j.colsurfa.2014.10.031**.

36 H. Ahmad, N. H. Abdul Kahar, R. Ramli, N. Yusoff, S. A. Reduan, M. F. Ismail, K. S. Lim, W. Y. Chong and M. Yasin, The performance of Ti_2C MXene and Ti_2AlC MAX Phase as saturable absorbers for passively mode-locked fiber laser, *Opt. Fiber Technol.*, 2021, **67**, 102683, DOI: **10.1016/j.yofte.2021.102683**.

37 M. Tang, J. Li, Y. Wang, W. Han, S. Xu, M. Lu, W. Zhang and H. Li, Surface terminations of MXene: synthesis, characterization, and properties, *Symmetry*, 2022, **14**, 2232, DOI: **10.3390/sym14112232**.

38 T. Ramani, K. Leon Prasanth and B. Sreedhar, Air stable colloidal copper nanoparticles: Synthesis, characterization and their surface-enhanced Raman scattering properties, *Phys. E*, 2016, **77**, 65–71, DOI: **10.1016/j.physe.2015.11.002**.

39 C. Madhusha, T. Jayasundara, I. Munaweera, C. Perera, G. Wijesinghe, M. Weerasekera, C. Sandaruwan, A. Meiyazhagan, F. C. Robles Hernandez, P. M. Ajayan and N. Kottegoda, Synthesis and structural characterization of copper nanoparticles doped activated carbon derived from coconut coir for drinking water purification, *Mater. Today Chem.*, 2023, **27**, 101312, DOI: **10.1016/j.mtchem.2022.101312**.

40 M. Mustakeem, J. K. El-Demellawi, M. Obaid, F. Ming, H. N. Alshareef and N. Ghaffour, MXene-Coated Membranes for Autonomous Solar-Driven Desalination, *ACS Appl. Mater. Interfaces*, 2022, **14**, 5265–5274, DOI: **10.1021/acsami.1c20653**.

41 S. Chen, L. Brown, M. Levendorf, W. Cai, S. Ju and J. Edgeworth, Oxidation Resistance of Graphene-Coated Cu and Cu/Ni Alloy, *ACS Nano*, 2011, **5**, 1321–1327, DOI: **10.1021/nn103028d**.

42 S. N. Shoghl, J. Jamali and M. K. Moravezi, Electrical conductivity, viscosity, and density of different nanofluids: an experimental study, *Exp. Therm. Fluid Sci.*, 2016, **74**, 339–346, DOI: **10.1016/j.expthermflusci.2016.01.004**.

43 S. Das, A. Giri, S. Samanta and S. Kanagaraj, Role of graphene nanofluids on heat transfer enhancement in thermosyphon, *J. Sci.: Adv. Mater. Devices*, 2019, **4**, 163–169, DOI: **10.1016/j.jsamd.2019.01.005**.

44 M. R. Chandan, A. H. Shaik, H. Kumar, A. Rahaman, D. K. Bal, B. A. Ponnusami and M. Imran, Influence of polymer washing on thermal conductivity enhancement of Cu nanofluids, *Asia-Pac. J. Chem. Eng.*, 2020, **15**, e2501, DOI: **10.1002/apj.2501**.

45 J. Wohld, J. Beck, K. Inman, M. Palmer, M. Cummings, R. Fulmer and S. Vafaei, Hybrid Nanofluid Thermal Conductivity and Optimization: Original Approach and Background, *Nanomaterials*, 2022, **12**, 2847, DOI: **10.3390/nano12162847**.

46 L. Zhou, B. Wang, X. Peng, X. Du and Y. Yang, On the Specific Heat Capacity of CuO Nanofluid, *Adv. Mech. Eng.*, 2010, **2**, 172085, DOI: **10.1155/2010/172085**.

47 H. Adun, I. Wole-osho, E. C. Okonkwo, D. Kavaz and M. Dagbasi, A critical review of specific heat capacity of hybrid nanofluids for thermal energy applications, *J. Mol. Liq.*, 2021, **340**, 116890, DOI: **10.1016/j.molliq.2021.116890**.

48 R. R. Sahoo and V. Kumar, Development of a new correlation to determine the viscosity of ternary hybrid nanofluid, *Int. Commun. Heat Mass Transfer*, 2020, **111**, 104451, DOI: **10.1016/j.icheatmasstransfer.2019.104451**.

49 R. E. Simons, comparing heat transfer rates of liquid coolants using the Mouromtseff number, Calc, *Corner*, 2006, **12**, 10.

50 Z. Said, N. K. Cakmak, P. Sharma, L. S. Sundar, A. Inayat, O. Keklikcioglu and C. Li, Synthesis, stability, density, viscosity of ethylene glycol-based ternary hybrid nanofluids: Experimental investigations and model-prediction using modern machine learning techniques, *Powder Technol.*, 2022, **400**, 117190, DOI: **10.1016/j.powtec.2022.117190**.

51 R. B. Abernethy, R. P. Benedict and R. B. Dowdell, Asme Measurement Uncertainty, *Am. Soc. Mech. Eng.*, 1985, **107**, 161.